

Error bounds for dynamical spectral estimation

Robert J. Webber*, Erik H. Thiede†, Douglas Dow‡, Aaron R. Dinner†, and Jonathan Weare‡

Abstract. Dynamical spectral estimation is a well-established numerical approach for estimating eigenvalues and eigenfunctions of the Markov transition operator from trajectory data. Dynamical spectral estimation has been applied for two decades in biomolecular simulation, yet its error properties remain poorly understood. Here we analyze the error of a dynamical spectral estimation method called “the variational approach to conformational dynamics” (VAC). We bound the approximation error and estimation error for VAC estimates. Our analysis establishes VAC’s convergence properties and suggests a new approach for tuning the lag time to improve VAC accuracy.

Key words. transition operator, Rayleigh-Ritz method, Markov state models, computational statistical mechanics, conformation dynamics

AMS subject classifications. 65C05, 60J35, 65N30

1. Introduction. An essential goal in simulation studies is identifying functions that decorrelate slowly in time. Slowly decorrelating functions are important for dimensionality reduction and prediction, since the values of these functions can be forecast far into the future. Moreover, because of their persistent nature, slowly decorrelating functions often have scientific significance. For example, in biomolecular systems, arrangements that control biological activity generally decorrelate very slowly compared to small fluctuations of bond lengths and angles.

Dynamical spectral estimation is a numerical approach that uses simulated trajectories to estimate the eigenvalues and eigenfunctions of the Markov transition operator. Under appropriate assumptions, a small number of eigenfunctions span all the most slowly decorrelating functions of the system, and the eigenvalues determine the slowest decorrelation rates. Therefore, dynamical spectral estimation is a rigorous approach for estimating slowly decorrelating functions.

Despite the prevalence of dynamical spectral estimation in biomolecular simulation studies, estimated eigenfunctions and eigenvalues can have substantial error [42], and the cause of this error is not yet fully understood. Our goal here is to identify and bound the major error sources, thereby identifying opportunities where dynamical spectral estimation can produce accurate results.

We focus on a dynamical spectral estimation method called “the variational approach to conformational dynamics” (VAC) [26, 5, 25, 12]. VAC can be applied to any Markov process X_t that is ergodic and reversible with respect to a distribution μ . After gathering data by simulating X_t , VAC consists of two steps. First, simulation data is used to estimate

* Courant Institute of Mathematical Sciences, New York University, New York, NY (rw2515@nyu.edu, weare@nyu.edu).

† Department of Chemistry, University of Chicago, Chicago, IL (thiede@uchicago.edu, dinner@uchicago.edu).

‡ Department of Mathematics, University of Chicago, Chicago, IL (ddow11@uchicago.edu).

expectations $C_{ij}(\tau) = \mathbb{E}_\mu[\phi_i(X_0)\phi_j(X_\tau)]$ for a set of basis functions $(\phi_i)_{1 \leq i \leq n}$. Second, the spectral decomposition of the matrix $C(0)^{-1}C(\tau)$ is used to estimate eigenvalues and eigenfunctions of the transition operator of X_t .

Our mathematical analysis establishes bounds on VAC's approximation error and estimation error. *Approximation error* is the theoretical approximation quality of VAC if expectations $C_{ij}(\tau) = \mathbb{E}_\mu[\phi_i(X_0)\phi_j(X_\tau)]$ were computed perfectly. *Estimation error* is the additional error incurred in VAC estimates because matrices $C(0)$ and $C(\tau)$ are computed imperfectly using a finite data set.

We are not the first authors to mathematically examine VAC's error. Djurdjevac and coauthors [7] bounded the approximation error of VAC eigenvalues. We extend their work by bounding the approximation error for VAC eigenfunctions, which are the chief objects of interest in most applications of dynamical spectral estimation. Additionally, we provide the first analysis of estimation error both for VAC eigenvalues and for eigenfunctions.

The analysis of VAC is challenging and requires original mathematics. We find that the standard bounds for the approximation of eigenspaces (e.g., [35, pg. 103] or [17, pg. 990]) are not sufficiently detailed to show how approximation error depends on the lag time parameter τ . A major contribution of our work is to use the structure of the transition operator at long lag times to obtain sharp error bounds. These new bounds successfully demonstrate the benefit of long lag times for reducing approximation error.

Our error bounds draw attention to a subtle conditioning problem that has not been fully explained in past work. VAC is error-prone at short lag times due to the high approximation error and also at long lag times due to the high estimation error. Therefore, it is best to select an intermediate lag time.

While our analysis does not fully determine the Goldilocks lag time that minimizes error, we offer diagnostic tools to help measure error levels and rule out lag times that are excessively high. One diagnostic, the *VAC eigenvalue ratio*, identifies the range of lag times during which approximation error must decrease and then stabilize. A second diagnostic, the *asymptotic estimation error*, identifies the estimation error from data by using asymptotic formulas. In experiments we find that these new diagnostic tools make it possible to measure error with greater accuracy compared to the previous leading approach [42].

The paper is organized as follows. Background material is given in [section 2](#), theoretical results are in [section 3](#), numerical experiments are in [section 4](#), mathematical derivations are in [section 5](#), and the conclusions follow in [section 6](#).

2. Background. This section presents background material explaining the VAC algorithm and the dynamical quantities VAC approximates.

2.1. VAC. We begin by introducing the steps of VAC applied to a process X_t with an ergodic, reversible distribution μ . The algorithm starts by estimating expectations involving a set of basis functions $(\phi_i)_{1 \leq i \leq n}$. Subsequently, VAC solves an eigenvalue problem involving matrices of expectations.

In [Algorithm 2.1](#), we are purposefully vague about the exact method for obtaining the estimates

$$(2.1) \quad \hat{C}_{ij}(\tau) \approx C_{ij}(\tau) = \mathbb{E}_\mu[\phi_i(X_0)\phi_j(X_\tau)].$$

Algorithm 2.1 VAC algorithm at lag time τ .

1. Form matrix $\hat{C}(0)$ with entries $\hat{C}_{ij}(0) \approx C_{ij}(0) = E_\mu[\phi_i(X_0)\phi_j(X_0)]$.
2. Form matrix $\hat{C}(\tau)$ with entries $\hat{C}_{ij}(\tau) \approx C_{ij}(\tau) = E_\mu[\phi_i(X_0)\phi_j(X_\tau)]$.
3. Solve eigenvalue problem $\hat{\lambda}_i^\tau \hat{v}^i(\tau) = \hat{C}(0)^{-1} \hat{C}(\tau) \hat{v}^i(\tau)$.
4. Return VAC eigenvalues $\hat{\lambda}_i^\tau$ and VAC eigenfunctions $\hat{\gamma}_i^\tau = \sum_j \hat{v}_j^i(\tau) \phi_j$.

One common approach involves simulating long trajectories of X_t and removing the start of each trajectory to limit equilibration bias [39]. A second common approach (“importance sampling” [19]) involves simulating short trajectories and addressing bias through an appropriate reweighting procedure [28, 50]. Since there are no restrictions on how the data set is generated, enhanced sampling techniques can be used to generate the trajectory initial conditions or even the trajectories themselves [3, 30].

In addition to collecting a data set, another key design feature affecting VAC is the choice of the basis functions. In the mid-1990s, early versions of VAC used the coordinate axes as basis functions [44, 10], a choice that remains common in molecular dynamics simulations [24, 38, 31]. Independently, in the late 1990s and early 2000s, researchers began constructing spectral estimates from “Markov state models” [37, 42, 43], a procedure mathematically equivalent to performing VAC using a basis of indicator functions on disjoint regions of state space. This idea of using a basis of indicator functions can be traced back to a publication by Stanislaw Ulam in 1960 [47, pg.74-75] and leads to simplifications in the eigenvalue problem in Algorithm 2.1. In the 2010s, it was observed that these schemes shared a common mathematical framework that could be extended to arbitrary basis sets [26]. Subsequent work led to the development of new families of basis functions [29, 48, 2, 27].

The name “variational approach to conformational dynamics” is inspired by the min-max principle for self-adjoint operators [26, 33]. This variational principle demonstrates that eigenfunctions η of the transition operator maximize the value of the autocorrelation function

$$(2.2) \quad \rho_\eta(\tau) = \text{corr}_\mu[\eta(X_0), \eta(X_\tau)]$$

at all lag times $\tau > 0$. Consistent with this variational principle, VAC constructs linear combinations of basis functions that maximize autocorrelations. A recent approach due to [20] and [4] extends the linear fitting procedure in VAC by using artificial neural networks to form nonlinear combinations of basis functions that maximize autocorrelations. However, in the present analysis we focus on the linear VAC algorithm as described in Algorithm 2.1, and we leave analysis of the nonlinear fitting procedure to future work.

To help clarify the relationship between VAC and other related algorithms, we observe that the computational steps in Algorithm 2.1 can be used for many purposes which may be different from the goals of VAC. For example, AMUSE [46, 23] uses the same computational procedure as Algorithm 2.1, but the goal is to solve the blind-source separation problem in signal processing. Likewise, dynamic mode decomposition [34] and extended dynamic mode decomposition [49] use the same computational procedure as Algorithm 2.1, but the goal is to analyze *non-reversible* processes, particularly deterministic fluid flows. While the underlying computations are similar in all these cases, VAC refers specifically to the spectral estimation

of time-reversible processes. To learn more about the connections between VAC and other related algorithms, we refer the reader to the helpful review paper by Klus and coauthors [15].

2.2. Spectral theory. In this subsection, we take a closer look at the transition operator of the process X_t and its eigenfunctions. We assume X_t is either a continuous-time Feller process [13] or a discrete-time process restricted to the even lag times $t = 0, 2, 4, \dots$. We assume X_t is ergodic and time-reversible with respect to a distribution μ . Lastly, we use $\langle \cdot, \cdot \rangle$ to denote the inner product on the Hilbert space $L^2(\mu)$, and we set $\|\cdot\| = \langle \cdot, \cdot \rangle^{1/2}$.

The transition operator, also called the Koopman operator, is defined as the conditional expectation operator [13]

$$(2.3) \quad T_t[f](x) = \mathbb{E}[f(X_t) | X_0 = x].$$

There are three main properties of the transition operator that determine information about its eigenfunctions.

1. The transition operator T_t is self-adjoint in $L^2(\mu)$. The self-adjointness follows from the time-reversibility condition

$$(2.4) \quad \mu(dx) p_t(x, dy) = \mu(dy) p_t(y, dx), \quad \forall x, y,$$

where $p_t(x, dy)$ denotes the transition probabilities for the process X_t . By integrating over equation (2.4), we verify the self-adjointness property

$$(2.5) \quad \langle f, T_t g \rangle = \langle T_t f, g \rangle, \quad \forall f, g \in L^2(\mu).$$

2. The transition operator satisfies the *semigroup property*

$$(2.6) \quad T_{t+s} = T_t T_s.$$

For discrete-time processes, the semigroup property guarantees a decomposition

$$(2.7) \quad T_t = (T_1)^t \quad \forall t = 0, 1, 2, \dots$$

For continuous-time Feller processes, the decomposition can be extended even further, leading to the formula

$$(2.8) \quad T_t = e^{tA}, \quad \forall t \geq 0,$$

which relates the semigroup T_t to its *infinitesimal generator* A [13].

3. The transition operator is nonnegative

$$(2.9) \quad \langle f, T_t f \rangle = \langle T_{t/2} f, T_{t/2} f \rangle \geq 0, \quad \forall f \in L^2(\mu),$$

for all $t \geq 0$ if X_t is a continuous-time process and for $t = 0, 2, 4, \dots$ if X_t is a discrete-time process.

Using the spectral theorem for self-adjoint operators [32], we obtain a decomposition of either $-A$ or T_2 and we extend this decomposition to the transition operator T_t at lag times $t \geq 0$ or $t = 0, 2, 4, \dots$. The spectral decomposition takes the form

$$(2.10) \quad T_t = \int_0^\infty e^{-\sigma t} \Pi(d\sigma)$$

where $\Pi(d\sigma)$ is a projection-valued measure.

The spectral decomposition completely determines the time correlations of the process X_t . In particular, if the spectrum is discrete, then a finite set of orthonormal eigenfunctions are responsible for all the slowest decorrelations of the process X_t . However, if the spectrum is continuous near $\sigma = 0$, there is an infinite set of orthonormal functions that decorrelate arbitrarily slowly.

To avoid the possibility of having a continuous spectrum near $\sigma = 0$, it is sufficient to assume T_t is compact. Under compactness, the spectral decomposition takes the form

$$(2.11) \quad T_t = \sum_{i=1}^{\infty} e^{-\sigma_i t} \text{proj}[\eta_i],$$

where $e^{-\sigma_1 t} > e^{-\sigma_2 t} \geq e^{-\sigma_3 t} \geq \dots$ are eigenvalues, $\eta_1, \eta_2, \eta_3, \dots$ are eigenfunctions, and $\text{proj}[\eta_i]$ is the orthogonal projection onto the subspace spanned by η_i . By the ergodicity assumption, $e^{-\sigma_1 t} = 1$ is a simple eigenvalue of T_t corresponding to the eigenfunction $\eta_1 = 1$. Figure 1 shows additional examples of eigenfunctions for a compact transition operator T_t .

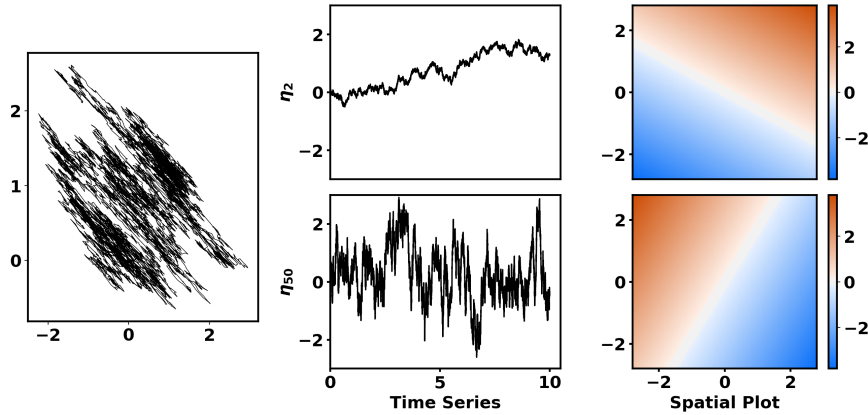


Figure 1: Eigenfunctions of a compact transition operator, corresponding to dynamics

$$d \begin{pmatrix} X \\ Y \end{pmatrix} = \begin{pmatrix} -0.4 & 0.17 \\ 0.17 & -0.2 \end{pmatrix} \begin{pmatrix} X \\ Y \end{pmatrix} dt + \sqrt{2} d \begin{pmatrix} W_1 \\ W_2 \end{pmatrix}.$$

Left: typical trajectory of (X_t, Y_t) . Upper middle: time series for eigenfunction η_2 with long decorrelation timescale $\sigma_2^{-1} = 5$. Lower middle: time series for eigenfunction η_{50} with short decorrelation timescale $\sigma_{50}^{-1} = 0.1$. Right: spatial structure of η_2 and η_{50} .

While the compactness assumption is enough to facilitate a rigorous analysis of VAC, the compactness assumption can be very restrictive. In the Monte Carlo literature, there are numerous examples of time-reversible processes with transition operators that are not compact such as the transition operator for the Metropolis-Hastings sampler [22, 1]. Therefore, we prefer to use the quasi-compactness assumption, a weaker assumption satisfied by a broader class of processes.

Assumption 2.1 (Quasi-compactness). The spectral decomposition for the transition operator T_t takes the form

$$(2.12) \quad T_t = \sum_{i=1}^r e^{-\sigma_i t} \text{proj}[\eta_i] + R_t, \quad R_t = \int_{[\sigma_{r+1}, \infty)} e^{-\sigma t} \Pi(d\sigma),$$

where $\eta_1, \eta_2, \dots, \eta_r$ are eigenfunctions, $e^{-\sigma_1 t} > e^{-\sigma_2 t} \geq \dots \geq e^{-\sigma_r t}$ are eigenvalues, and $e^{-\sigma_{r+1} t}$ is not necessarily an eigenvalue but it bounds the operator norm of the residual operator, that is, $\|R_t\|_2 \leq e^{-\sigma_{r+1} t}$.

Remark 2.2. In the analysis to follow, an “eigenspace” of T_t denotes the closed linear subspace of eigenfunctions with a given eigenvalue. A “simple eigenvalue” has a one-dimensional eigenspace. An “invariant subspace” \mathcal{U} is any closed linear subspace satisfying $T_t \mathcal{U} \subseteq \mathcal{U}$.

Remark 2.3. There is a common modification of Algorithm 2.1 where the estimated mean $\hat{\mu}_i \approx \mu_i = \mathbb{E}_\mu[\phi_i(X_0)]$ is subtracted from each one of the basis functions ϕ_i before performing VAC (see the discussion in [15]). When the mean is removed, VAC no longer estimates the trivial eigenfunction $\eta_1 = 1$; however, VAC continues to estimate all other eigenspaces.

2.3. Approximation of eigenspaces. It is colloquially said that VAC approximates eigenvalues and eigenfunctions, but it is more correct to say that VAC approximates eigenvalues and *eigenspaces*. Recall that $\hat{\lambda}_i^\tau$ and $\hat{\gamma}_i^\tau$ denote the VAC eigenvalues and eigenfunctions, while $e^{-\sigma_i \tau}$ and η_i are the true eigenvalues and eigenfunctions of the transition operator. We assume that VAC eigenvalues are arranged from largest to smallest so that $\hat{\lambda}_1^\tau \geq \hat{\lambda}_2^\tau \geq \dots \geq \hat{\lambda}_n^\tau$. Then VAC approximates eigenvalues

$$(2.13) \quad \hat{\lambda}_i^\tau \approx e^{-\sigma_i \tau}$$

for each $1 \leq i \leq n$. VAC approximates eigenspaces and other invariant subspaces

$$(2.14) \quad \text{span}_{j \leq i \leq k} \hat{\gamma}_i^\tau \approx \text{span}_{j \leq i \leq k} \eta_i,$$

whenever there is a gap between $\{\sigma_j, \dots, \sigma_k\}$ and all other σ_i values.

To measure the error in VAC subspaces, we introduce two distances: the gap distance $d_2(\cdot, \cdot)$ and the projection distance $d_F(\cdot, \cdot)$.

Definition 2.4. Consider closed subspaces \mathcal{U} and \mathcal{W} and let \mathcal{W}^\perp indicate the orthogonal complement of \mathcal{W} . Then, the gap distance and projection distance are defined by [8]

$$(2.15) \quad d_2(\mathcal{U}, \mathcal{W}) = \left\| \text{proj}[\mathcal{W}^\perp] \text{proj}[\mathcal{U}] \right\|_2, \quad d_F(\mathcal{U}, \mathcal{W}) = \left\| \text{proj}[\mathcal{W}^\perp] \text{proj}[\mathcal{U}] \right\|_F.$$

Here, $\|\cdot\|_2$ denotes the operator norm and $\|\cdot\|_F$ denotes the Hilbert-Schmidt norm, also known as the Frobenius norm.

The gap distance and projection distance are very flexible, and definitions (2.15) can be applied even if $\dim(\mathcal{U}) < \dim(\mathcal{W}) \leq \infty$. In this case, we observe that $d_2(\mathcal{U}, \mathcal{W})$ and $d_F(\mathcal{U}, \mathcal{W})$ are not technically distances. Rather, $d_2(\mathcal{U}, \mathcal{W})$ and $d_F(\mathcal{U}, \mathcal{W})$ are properly interpreted as distances between \mathcal{U} and the nearest $\dim(\mathcal{U})$ -dimensional subspace of \mathcal{W} .

We end this section by introducing a useful property of the projection distance that allows us to extend error bounds from a small range of subspaces to a wider range of subspaces when orthogonality conditions are satisfied.

Lemma 2.5. *Consider $\mathcal{U} = \text{span}(\mathcal{U}_1, \mathcal{U}_2)$ where \mathcal{U}_1 and \mathcal{U}_2 are orthogonal subspaces, and $\mathcal{W} = \text{span}(\mathcal{W}_1, \mathcal{W}_2)$ where \mathcal{W}_1 and \mathcal{W}_2 are orthogonal subspaces. Then,*

$$(2.16) \quad d_F^2(\mathcal{U}_2, \mathcal{W}_2) \leq d_F^2(\mathcal{U}, \mathcal{W}) + d_F^2(\mathcal{U}_1, \mathcal{W}_1).$$

Proof. Calculate

$$(2.17) \quad d_F^2(\mathcal{U}_2, \mathcal{W}_2) = \left\| \text{proj}[\mathcal{U}_2] \text{proj}[\mathcal{W}^\perp] \right\|_F^2 + \left\| \text{proj}[\mathcal{U}_2] \text{proj}[\mathcal{W}_1] \right\|_F^2$$

$$(2.18) \quad \leq \left\| \text{proj}[\mathcal{U}] \text{proj}[\mathcal{W}^\perp] \right\|_F^2 + \left\| \text{proj}[\mathcal{U}_1^\perp] \text{proj}[\mathcal{W}_1] \right\|_F^2$$

$$(2.19) \quad = d_F^2(\mathcal{U}, \mathcal{W}) + d_F^2(\mathcal{U}_1, \mathcal{W}_1) \quad \blacksquare$$

3. Theoretical results. To describe the approach taken in the theoretical analysis, we introduce an idealized VAC algorithm where expectations $C_{ij}(\tau) = \mathbb{E}_\mu[\phi_i(X_0)\phi_j(X_\tau)]$ and $C_{ij}(0) = \mathbb{E}_\mu[\phi_i(X_0)\phi_j(X_0)]$ are computed perfectly. Notationally, we distinguish between VAC and idealized VAC by using the hat symbol to indicate the quantities calculated using data. For VAC, we write $\hat{C}_{ij}(\tau)$, $\hat{\lambda}_i^\tau$, $\hat{v}^i(\tau)$, and $\hat{\gamma}_i^\tau$. For idealized VAC, we write $C_{ij}(\tau)$, λ_i^τ , $v^i(\tau)$, and γ_i^τ .

In the theoretical analysis, we use idealized VAC to isolate two different sources of error. We decompose subspace error using

$$(3.1) \quad \underbrace{d_F\left(\text{span}_{j \leq i \leq k} \hat{\gamma}_i^\tau, \text{span}_{j \leq i \leq k} \eta_i\right)}_{\text{total error}} \leq \underbrace{d_F\left(\text{span}_{j \leq i \leq k} \gamma_i^\tau, \text{span}_{j \leq i \leq k} \eta_i\right)}_{\text{approximation error}} + \underbrace{d_F\left(\text{span}_{j \leq i \leq k} \hat{\gamma}_i^\tau, \text{span}_{j \leq i \leq k} \gamma_i\right)}_{\text{estimation error}}.$$

Analogously, we decompose eigenvalue error using

$$(3.2) \quad \underbrace{\left| \hat{\lambda}_i^\tau - e^{-\sigma_i \tau} \right|}_{\text{total error}} \leq \underbrace{\left| \lambda_i^\tau - e^{-\sigma_i \tau} \right|}_{\text{approximation error}} + \underbrace{\left| \hat{\lambda}_i^\tau - \lambda_i^\tau \right|}_{\text{estimation error}}.$$

Approximation error is the difference between idealized VAC estimates and the true eigenvalues and eigenspaces. Estimation error is the difference between VAC estimates and idealized VAC estimates. We first present approximation error bounds in [subsection 3.1](#) and then we present estimation error bounds in [subsection 3.2](#).

Remark 3.1. Throughout the section, we use numerical experiments to illustrate the implications of the error bounds. [Figure 2](#), [Figure 3](#), and [Figure 4](#) all demonstrate the error of VAC when applied to the Ornstein-Uhlenbeck process $dX = -X dt + \sqrt{2} dW$ using a basis of indicator functions. Details on how the figures were generated appear in the supplement.

3.1. Approximation error. In this subsection, we first bound the approximation error by using traditional Rayleigh-Ritz approximation bounds. However, we find that the Rayleigh-Ritz bounds do not provide enough information to show how approximation error depends on the lag time parameter τ . Therefore, we derive improved bounds by using original methods. The improved bounds are asymptotically sharp at long lag times, revealing how long lag times cause the approximation error to stabilize.

3.1.1. Existing approximation bounds are inadequate. The idealized VAC algorithm is equivalent to the *Rayleigh-Ritz method* in spectral estimation. In the Rayleigh-Ritz method [41], the eigenvalues and eigenspaces of a target operator A are estimated by introducing a subspace of functions \mathcal{U} and then calculating the eigenvalues and eigenspaces of $\text{proj}[\mathcal{U}] A|_{\mathcal{U}}$ where $A|_{\mathcal{U}}$ denotes the restriction of A to the subspace \mathcal{U} . This is also exactly what is done in idealized VAC. The target operator is the transition operator T_τ , and the subspace of basis functions is $\Phi = \text{span}_{1 \leq i \leq n} \phi_i$. Moreover, the idealized VAC eigenfunctions γ_i^τ are eigenfunctions of $\text{proj}[\Phi] T_\tau|_{\Phi}$ with eigenvalues λ_i^τ .

The equivalence between the Rayleigh-Ritz method and idealized VAC is known in the VAC literature [36, 7]. However, the implications for VAC's approximation error have not yet been fully explored. Djurdjevac and coauthors [7] applied Rayleigh-Ritz error bounds to analyze idealized VAC eigenvalues. The following theorem takes a step further, by also applying Rayleigh-Ritz error bounds to analyze idealized VAC eigenspaces.

Theorem 3.2 (Approximation bounds).

1. In the limit as $d_F(\text{span}_{1 \leq i \leq k} \eta_i, \Phi) \rightarrow 0$, idealized VAC eigenvalues converge

$$(3.3) \quad \lambda_i^\tau \rightarrow e^{-\sigma_i \tau}.$$

2. Eigenvalue approximation error is bounded by

$$(3.4) \quad 1 - d_2^2 \left(\text{span}_{1 \leq i \leq k} \eta_i, \Phi \right) \leq \frac{\lambda_k^\tau}{e^{-\sigma_k \tau}} \leq 1.$$

3. In the limit as $d_F(\text{span}_{1 \leq i \leq k} \eta_i, \Phi) \rightarrow 0$, idealized VAC subspaces converge

$$(3.5) \quad \text{span}_{j \leq i \leq k} \gamma_i^\tau \rightarrow \text{span}_{j \leq i \leq k} \eta_i,$$

provided there is a gap between $\{\sigma_j, \dots, \sigma_k\}$ and other σ_i values.

4. Subspace approximation error is bounded by

$$(3.6) \quad 1 \leq \frac{d_F^2(\text{span}_{1 \leq i \leq k} \gamma_i^\tau, \text{span}_{1 \leq i \leq k} \eta_i)}{d_F^2(\text{span}_{1 \leq i \leq k} \eta_i, \Phi)} \leq 1 + \frac{\|\text{proj}[\Phi^\perp] T_\tau \text{proj}[\Phi]\|_2^2}{|e^{-\sigma_k \tau} - \lambda_{k+1}^\tau|^2},$$

provided that $e^{-\sigma_k \tau} > \lambda_{k+1}^\tau$.

Proof. See [16, 17] for the original proofs, or see the derivations in the supplement. ■

The main takeaway from [Theorem 3.2](#) is that the approximation error converges to zero in the limit as

$$(3.7) \quad d_F \left(\text{span}_{1 \leq i \leq k} \eta_i, \Phi \right) \rightarrow 0.$$

Condition (3.7) implies that the basis set Φ must become very rich, so that eigenfunctions η_i can be closely approximated using linear combinations of basis functions.

The Rayleigh-Ritz error bound (3.6) clearly identifies how the eigenspace approximation error must decay with an increasingly rich basis. However, the bound is not sufficiently detailed to identify how approximation error depends on the lag time τ . As seen in [Figure 2](#), the Rayleigh-Ritz bound (3.6) asymptotes to infinity as the lag time increases, implying that approximation error can grow arbitrarily large. In contrast to this upper bound, however, experiments reveal that approximation error decreases and then stabilizes as the lag time tends to infinity. In the next section, we will derive an improved bound that is asymptotically sharp, describing the exact behavior of the approximation error as $\tau \rightarrow \infty$.

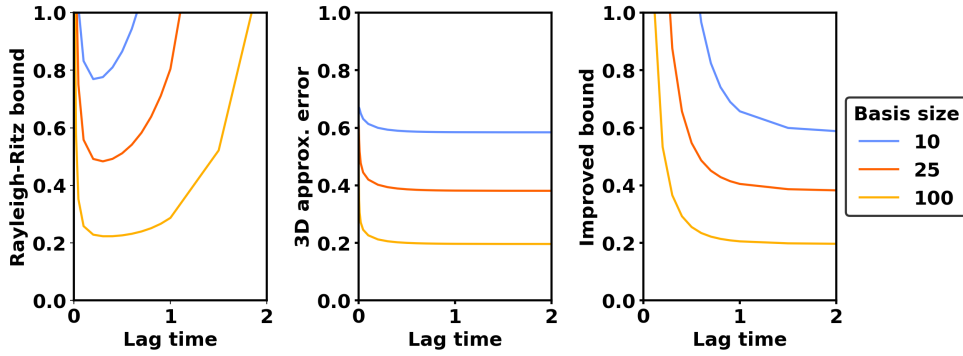


Figure 2: Left: the Rayleigh-Ritz bound asymptotes to infinity at long and short lag times. Center: the true approximation error stabilizes at long lag times. Right: the improved bound presented in [Theorem 3.4](#) is asymptotically sharp at long lag times. Here, 3D approximation error is the projection distance between $\text{span}_{1 \leq i \leq 3} \gamma_i^\tau$ and $\text{span}_{1 \leq i \leq 3} \eta_i$.

3.1.2. New approximation bounds. To analyze the dependence on lag time, we develop a mathematical approach different from the methods applied to the Rayleigh-Ritz method in the past. We start by identifying a key stability property of idealized VAC that has not appeared in the previous literature. As $\tau \rightarrow \infty$, idealized VAC eigenvalues and eigenspaces converge to a well-defined limit. This convergence implies that the approximation error must stabilize at long lag times.

To rigorously study the convergence of idealized VAC estimates, our first step is to introduce the orthogonalized projection functions q_1, q_2, \dots . These are the natural functions to appear in the $\tau \rightarrow \infty$ limit. They are constructed from the projected eigenfunctions $\text{proj}[\Phi] \eta_1, \text{proj}[\Phi] \eta_2, \dots$, but they are adjusted to meet the orthogonality constraints on idealized VAC eigenfunctions.

Definition 3.3. Set $p = \min \{n, r\}$, where n is the number of basis functions $(\phi_i)_{1 \leq i \leq n}$ and r is the number of eigenfunctions $(\eta_i)_{1 \leq i \leq r}$. Assume that projections $\text{proj}[\Phi] \eta_i$ are linearly independent for $1 \leq i \leq p$. Then, define

$$(3.8) \quad \tilde{q}_1 = \text{proj}[\Phi] \eta_1, \quad q_1 = \tilde{q}_1 / \|\tilde{q}_1\|.$$

$$(3.9) \quad \tilde{q}_2 = \text{proj}[\Phi] \eta_2 - \langle q_1, \eta_2 \rangle q_1, \quad q_2 = \tilde{q}_2 / \|\tilde{q}_2\|.$$

$$(3.10) \quad \vdots$$

$$(3.11) \quad \tilde{q}_p = \text{proj}[\Phi] \eta_p - \sum_{i=1}^{p-1} \langle q_i, \eta_p \rangle q_i, \quad q_p = \tilde{q}_p / \|\tilde{q}_p\|.$$

Our next step is to prove that idealized VAC eigenfunctions γ_i^τ converge to the orthogonalized projections q_i at long lag times.

Theorem 3.4 (The $\tau \rightarrow \infty$ limit).

1. In the limit as $\tau \rightarrow \infty$, idealized VAC eigenvalues converge

$$(3.12) \quad \frac{\lambda_i^\tau}{e^{-\sigma_i \tau}} \rightarrow \langle \eta_i, q_i \rangle^2,$$

provided there is a gap between σ_i and other σ_j values.

2. In the limit as $\tau \rightarrow \infty$, idealized VAC subspaces converge

$$(3.13) \quad \text{span}_{j \leq i \leq k} \gamma_i^\tau \rightarrow \text{span}_{j \leq i \leq k} q_i,$$

provided there is a gap between $\{\sigma_j, \dots, \sigma_k\}$ and other σ_i values.

3. In the limit as $\tau \rightarrow \infty$, the convergence rate for idealized VAC eigenfunctions is

$$(3.14) \quad d_F \left(\text{span}_{1 \leq i \leq k} \gamma_i^\tau, \text{span}_{1 \leq i \leq k} q_i \right) = \left| \frac{\langle \eta_{k+1}, q_k \rangle}{\langle \eta_{k+1}, q_{k+1} \rangle} \right| \frac{\lambda_{k+1}^\tau}{\lambda_k^\tau} (1 + o(1)),$$

provided $e^{-\sigma_k \tau}$ and $e^{-\sigma_{k+1} \tau}$ are simple eigenvalues and $\langle \eta_{k+1}, q_k \rangle \neq 0$.

4. VAC's approximation error is bounded by

$$(3.15) \quad 1 \leq \frac{d_F^2(\text{span}_{1 \leq i \leq k} \gamma_i^\tau, \text{span}_{1 \leq i \leq k} \eta_i)}{d_F^2(\text{span}_{1 \leq i \leq k} \eta_i, \Phi)} \leq 1 + \frac{1}{4} \left| \frac{e^{-\sigma_{k+1} \tau}}{\lambda_k^\tau - e^{-\sigma_{k+1} \tau}} \right|^2,$$

provided that $e^{-\sigma_{k+1} \tau} < \lambda_k^\tau$.

Proof. See subsection 5.2, subsection 5.3, and subsection 5.4. ■

The main message of Theorem 3.4 is that idealized VAC eigenspaces converge exponentially fast as $\tau \rightarrow \infty$. Because of this convergence, the approximation error must stabilize.

Interpreting the results of Theorem 3.4 further, we can identify concrete strategies for how best to reduce approximation error. The approximation error can be divided into two parts:

$$(3.16) \quad \underbrace{d_F \left(\text{span}_{j \leq i \leq k} \gamma_i^\tau, \text{span}_{j \leq i \leq k} \eta_i \right)}_{\text{approximation error}} \leq \underbrace{d_F \left(\text{span}_{j \leq i \leq k} q_i, \text{span}_{j \leq i \leq k} \eta_i \right)}_{\text{lag-time-independent error}} + \underbrace{d_F \left(\text{span}_{j \leq i \leq k} \gamma_i^\tau, \text{span}_{j \leq i \leq k} q_i \right)}_{\text{lag-time-dependent error}}.$$

In this decomposition, we separate the lag-time-independent error and the lag-time-dependent error. In applications of VAC, there are separate strategies for reducing these two error sources.

To reduce the lag-time-independent error, the best strategy is to enrich the basis set as much as possible. If the basis set is rich enough to approximate the top eigenfunctions $\eta_1, \eta_2, \dots, \eta_k$ with high accuracy, then the lag-time-independent error must be low. Assuming there is a gap between $\{\sigma_j, \dots, \sigma_k\}$ and other σ_i values, [Lemma 2.5](#) guarantees

$$(3.17) \quad \underbrace{d_F^2 \left(\text{span}_{j \leq i \leq k} q_i, \text{span}_{j \leq i \leq k} \eta_i \right)}_{\text{squared lag-time-independent error}} \leq d_F^2 \left(\text{span}_{1 \leq i \leq j-1} \eta_i, \Phi \right) + d_F^2 \left(\text{span}_{1 \leq i \leq k} \eta_i, \Phi \right).$$

Sharper bounds on the lag-time-independent error are also presented in the supplement.

To reduce the lag-time-dependent error, the best strategy is simply to increase the lag time. As $\tau \rightarrow \infty$, the lag-time-dependent error decays exponentially fast in proportion to $e^{-(\sigma_{k+1}-\sigma_k)\tau}$. Given a sufficiently rich data set, the *VAC eigenvalue ratio*

$$(3.18) \quad \hat{\lambda}_{k+1}^\tau / \hat{\lambda}_k^\tau$$

also decays in proportion to $e^{-(\sigma_{k+1}-\sigma_k)\tau}$. As seen in [Figure 3](#), the VAC eigenvalue ratio helps identify the asymptotic convergence rate for the lag-time-dependent error. However, at short lag times, the lag-time-dependent error can decay more quickly than $e^{-(\sigma_{k+1}-\sigma_k)\tau}$ due to preasymptotic error sources.

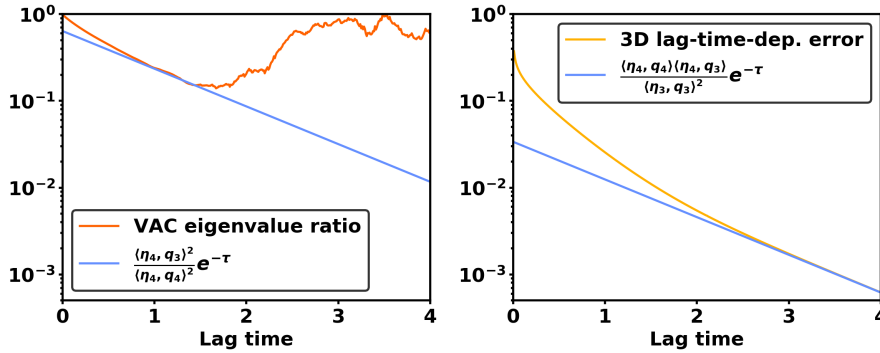


Figure 3: When estimation error is low, VAC eigenvalue ratio decays in proportion to $e^{-(\sigma_4-\sigma_3)\tau}$ (left). At long lag times, lag-time-dependent error also decays in proportion to $e^{-(\sigma_4-\sigma_3)\tau}$ (right), but it decays more quickly at short lag times.

In experiments, we find it is best to interpret the VAC eigenvalue ratio as a theoretical upper bound. When the VAC eigenvalue ratio is small, it provides a guarantee that a large part of the lag-time-dependent error has been eliminated. Conversely, when the VAC eigenvalue ratio is nearly one, users should be wary that VAC estimates are potentially contaminated by lag-time-dependent error.

3.2. Estimation error. In this subsection, we present formulas for the estimation error and explain how to calculate the typical estimation error using data.

3.2.1. Formulas for the estimation error. In applications of VAC, it is not typically possible to evaluate expectations $C_{ij}(\tau) = \mathbb{E}_\mu[\phi_i(X_0)\phi_j(X_\tau)]$ exactly. Instead, stochastic simulation is used to provide estimates $\hat{C}_{ij}(\tau) \approx C_{ij}(\tau)$. In the asymptotic limit as $\hat{C}(\tau) \rightarrow C(\tau)$ and $\hat{C}(0) \rightarrow C(0)$, the estimation error is governed by the following asymptotic formulas.

Theorem 3.5 (Estimation error). *Assume idealized VAC eigenfunctions are normalized so that $\langle \gamma_i^\tau, \gamma_j^\tau \rangle = \delta_{ij}$, and recall v_i^τ is the vector with $\gamma_i^\tau = \sum_{j=1}^n v_j^i(\tau) \phi_j$. Set*

$$(3.19) \quad \hat{L}_{li}(\tau) = v_l(\tau)^T \left[\hat{C}(\tau) - \lambda_i^\tau \hat{C}(0) \right] v_i(\tau), \quad 1 \leq l, i \leq n$$

1. As $\hat{C}(\tau) \rightarrow C(\tau)$ and $\hat{C}(0) \rightarrow C(0)$, eigenvalue estimation error is described by

$$(3.20) \quad \hat{\lambda}_i^\tau - \lambda_i^\tau = \hat{L}_{ii}(\tau) + \mathcal{O}\left(\left\|\hat{C}(\tau) - C(\tau)\right\|_F^2 + \left\|\hat{C}(0) - C(0)\right\|_F^2\right),$$

provided there is a gap between λ_i^τ and all other idealized eigenvalues.

2. As $\hat{C}(\tau) \rightarrow C(\tau)$ and $\hat{C}(0) \rightarrow C(0)$, subspace estimation error is described by

$$(3.21) \quad d_F\left(\text{span}_{j \leq i \leq k} \hat{\gamma}_i^\tau, \text{span}_{j \leq i \leq k} \gamma_i^\tau\right) = \left(\sum_{i=j}^k \sum_{\substack{l < j \\ \text{or } l > k}} \left|\frac{\hat{L}_{li}(\tau)}{\lambda_l^\tau - \lambda_i^\tau}\right|^2\right)^{1/2} + \mathcal{O}\left(\left\|\hat{C}(\tau) - C(\tau)\right\|_F^2 + \left\|\hat{C}(0) - C(0)\right\|_F^2\right),$$

provided there is a gap between $\{\lambda_j^\tau, \dots, \lambda_k^\tau\}$ and all other idealized eigenvalues.

3. The condition number for VAC subspaces is given by

$$(3.22) \quad \limsup_{\substack{\hat{C}(\tau) \rightarrow C(\tau) \\ \hat{C}(0) \rightarrow C(0)}} \frac{d_F\left(\text{span}_{j \leq i \leq k} \hat{\gamma}_i^\tau, \text{span}_{j \leq i \leq k} \gamma_i^\tau\right)}{\left\|\hat{L}(\tau)\right\|_F} = \frac{1}{\min\left\{\lambda_{j-1}^\tau - \lambda_j^\tau, \lambda_k^\tau - \lambda_{k+1}^\tau\right\}}.$$

with the conventions $\lambda_0^\tau = \infty$ and $\lambda_{n+1}^\tau = -\infty$.

Proof. See [subsection 5.5](#). ■

A useful quantity identified in [Theorem 3.5](#) is the *condition number* [40]. The condition number quantifies VAC's sensitivity to small errors in the matrices $\hat{C}(\tau)$ and $\hat{C}(0)$. In experiments, we find the condition number is a useful heuristic for judging whether a VAC estimation problem is easy or hard—more specifically whether a large or small data set is required for accurate estimation. As the condition number reaches high values like 10, 25, or 100, VAC estimates are increasingly likely to be contaminated by estimation error. Empirically, the condition number can be estimated using

$$(3.23) \quad \min\left\{\hat{\lambda}_{j-1}^\tau - \hat{\lambda}_j^\tau, \hat{\lambda}_k^\tau - \hat{\lambda}_{k+1}^\tau\right\}^{-1}.$$

3.2.2. Calculating the typical estimation error using data. Here, we explain how to calculate the typical estimation error using trajectory data. We assume for simplicity that the data consists of a single long equilibrium trajectory of the process X_t . However, the estimation procedure described here could be generalized to other types of trajectory data.

Our approach for calculating the typical estimation error is based on the following asymptotic characterization.

Theorem 3.6. *Assume $E_\mu |\phi_i(X_0)|^4 < \infty$ for $1 \leq i \leq n$. Assume an equilibrium trajectory $X_0, X_\Delta, X_{2\Delta}, \dots, X_{T-\Delta}$ is simulated and estimates $\hat{C}_{ij}(\tau)$ are formed using*

$$(3.24) \quad \hat{C}_{ij}(\tau) = \frac{\Delta}{T-\tau} \sum_{s=0}^{\frac{T-\tau}{\Delta}-1} \frac{\phi_i(X_{s\Delta}) \phi_j(X_{s\Delta+\tau}) + \phi_j(X_{s\Delta}) \phi_i(X_{s\Delta+\tau})}{2}.$$

Then, as $T \rightarrow \infty$ the estimation error is characterized by

$$(3.25) \quad \sqrt{T} \left(\hat{\lambda}_i^\tau - \lambda_i^\tau \right) \xrightarrow{\mathcal{D}} Z_{ii}(\tau)$$

$$(3.26) \quad \sqrt{T} d_F \left(\text{span}_{j \leq i \leq k} \hat{\gamma}_i^\tau, \text{span}_{j \leq i \leq k} \gamma_i^\tau \right) \xrightarrow{\mathcal{D}} \sum_{i=j}^k \left(\sum_{\substack{l < j \\ \text{or } l > k}} \frac{Z_{li}(\tau)^2}{|\lambda_l^\tau - \lambda_i^\tau|^2} \right)^{1/2}.$$

Here, $(Z_{li}(\tau))_{1 \leq l, i \leq n}$ is a mean-zero multivariate normal distribution that satisfies

$$(3.27) \quad E |V_{li}(\tau)|^2 = \Delta \sum_{s=-\infty}^{\infty} \text{Cov}_\mu [F_{li}^\tau(X_0, X_\tau), F_{li}^\tau(X_{s\Delta}, X_{s\Delta+\tau})],$$

with

$$(3.28) \quad F_{li}^\tau(x, y) = \frac{\gamma_l^\tau(x) \gamma_i^\tau(y) + \gamma_l^\tau(y) \gamma_i^\tau(x)}{2} - \lambda_i^\tau \frac{\gamma_l^\tau(x) \gamma_i^\tau(x) + \gamma_l^\tau(y) \gamma_i^\tau(y)}{2}.$$

Proof. See subsection 5.6 ■

The great value of Theorem 3.6 is that it suggests a data-driven approach for calculating the asymptotic estimation error. First, the data set is used to provide asymptotic variance estimates $\hat{V}_{li}(\tau)^2 \approx E |Z_{li}(\tau)|^2$ by means of equation (3.27). Second, the estimates $\hat{V}_{li}(\tau)^2$ are substituted into equation (3.25) to compute the typical eigenvalue estimation error or equation (3.26) to compute the typical eigenspace estimation error. A complete description of this procedure appears in the supplement.

We refer to the calculated estimation error using Theorem 3.6 as the *asymptotic estimation error*. The asymptotic estimation error is empirically very accurate when estimation error levels are low, as seen in Figure 4. However, when estimation error levels are high, the asymptotic estimation error is no longer very accurate since the assumptions underlying the asymptotic formulas begin to fail.

We conclude this section by considering three strategies to reduce the estimation error of VAC. The first strategy is to increase trajectory length. By increasing the length T of the trajectory, the estimation error consistently decreases at a $1/\sqrt{T}$ rate as shown in Figure 4.

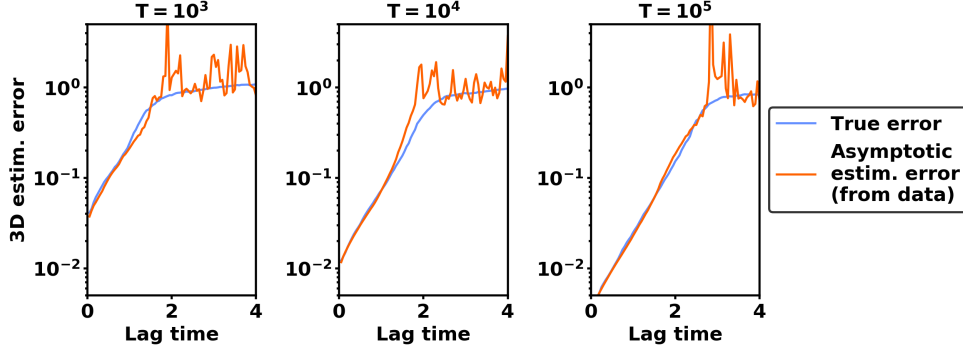


Figure 4: Estimation error for different trajectory lengths T . True error is the mean squared estimation error from 100 independent trials. The asymptotic estimation error is calculated during a single trial using formulas from [Theorem 3.6](#).

The second strategy for reducing the estimation error is to prune the size of the basis set. Examining the results of [Theorem 3.5](#), we find that the squared estimation error increases linearly with the number of basis functions. Therefore, it is best to include only those basis functions that have the potential to overlap with the eigenfunctions of the transition operator.

The final strategy for reducing the estimation error is to select basis functions with favorable integrability properties. In [Theorem 3.6](#), it is seen that the typical estimation error potentially depends on the fourth moments of the idealized VAC coordinates. If the basis functions themselves have large kurtosis

$$(3.29) \quad \frac{\mathbb{E}_\mu |\phi_i(X_0) - \mathbb{E}_\mu [\phi_i(X_0)]|^4}{\left(\mathbb{E}_\mu |\phi_i(X_0) - \mathbb{E}_\mu [\phi_i(X_0)]|^2\right)^2},$$

this can increase the fourth moments of the idealized VAC coordinates, contributing to the estimation error in VAC calculations. Integrability may be one factor that helps explain the success of Markov state models in which the basis consists of indicator functions. The higher moments of indicator functions are often well-controlled, compared to, e.g., higher order polynomials of the coordinate axes.

4. Numerical experiments. In this section, we report on two numerical experiments that illustrate the major factors impacting VAC accuracy.

4.1. Varying the basis size and trajectory length. First, we apply VAC to estimate the span of eigenfunctions η_1 , η_2 and η_3 for the Ornstein-Uhlenbeck (OU) process

$$(4.1) \quad dX = -X dt + \sqrt{2} dW.$$

In two different trials, we show how VAC's accuracy depends on the size of the basis set and the length of the simulated trajectory. The number of basis functions and the trajectory length are varied as follows:

	Trial 1	Trial 2
Basis functions	$n = 20$	$n = 50$
Trajectory length	$T = 10^4$	$T = 500$

In both trials, the basis functions are indicator functions on disjoint intervals.

The two different trials demonstrate that the breakdown of approximation error and estimation error is sensitive to context, as seen in Figure 5. The approximation error is higher in trial 1 because of the smaller library of basis functions, while the estimation error is higher in trial 2 because of the smaller data set. In trial 1, it is optimal to use a comparatively long lag time of $\tau = 0.7$. In contrast, in trial 2 it is optimal to use a comparatively short lag time of $\tau = 0.1$ to avoid the upsurge of estimation error at longer lag times.

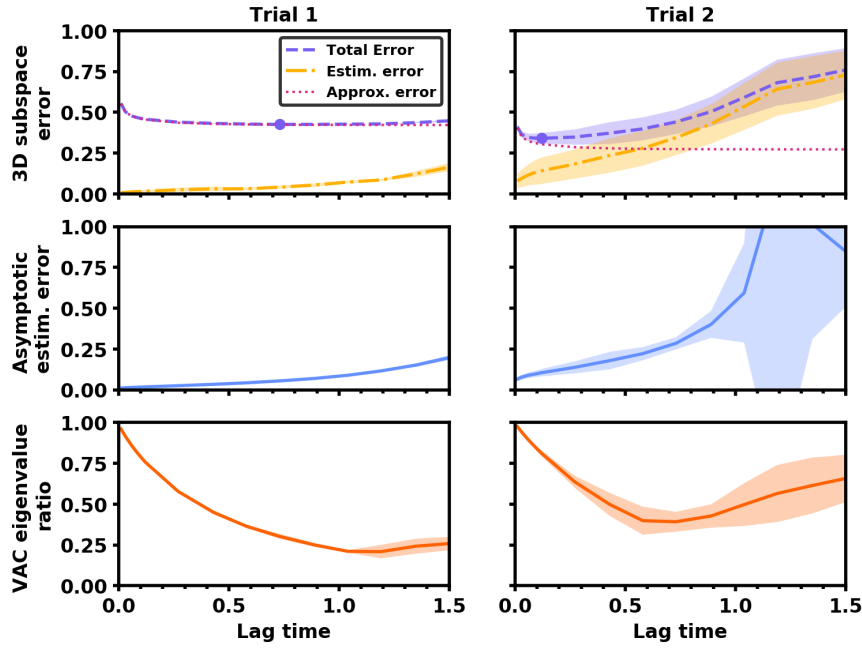


Figure 5: Top: total error is decomposed into estimation error and approximation error (top). Purple dot shows the minimum subspace error: the “optimal lag time.” Middle: asymptotic estimation error. Bottom: VAC eigenvalue ratio. Bold lines indicate the mean over 30 independent trajectories, while the shaded region indicates the mean ± 1 standard deviation.

In addition to showing the true error levels, Figure 5 shows two diagnostic tools that are computed directly from the data: the asymptotic estimation error and the VAC eigenvalue ratio. The asymptotic estimation error correctly identifies the rising levels of estimation error as the lag time increases. The VAC eigenvalue ratio correctly identifies the reduction in the approximation error as the lag time increases. Specifically, the VAC eigenvalue ratio decreases at a rate of $e^{-\tau}$, indicating that the approximation error stabilizes more quickly than $e^{-\tau}$ at short time lags and eventually converges at a rate of $e^{-\tau}$ at long time lags. The asymptotic estimation error and VAC eigenvalue ratio could be used to to partially measure the error

levels and to help select an appropriate lag time if the true error levels were unknown.

An alternative lag time selection strategy called “implied timescale analysis” has been advocated in the past by VAC researchers [42]. In this strategy, the VAC eigenvalues are used to compute the implied timescales

$$(4.2) \quad -\tau / \log(\hat{\lambda}_i^\tau).$$

If VAC eigenvalues are perfect estimates of the true eigenvalues, then implied timescales are perfectly flat and they equal σ_i^{-1} . In practice, however, implied timescales are not flat. They increase quickly at short lag times and then increase more slowly at long lag times. To cut down on VAC’s error, Swope and coauthors [42] proposed selecting a long enough lag time so that the implied timescales for the eigenfunctions of interest are approximately level.

Figure 6 presents the implied timescales for the OU process. From the figure it is clear that the implied timescales cannot be used to assess the estimation error. The estimation error is much higher in the second trial, yet the implied timescales for trial 1 and trial 2 are similar. However, implied timescales may help assess the approximation error. At a lag time of $\tau = 0.1$, the approximation error for the subspace $\{\eta_1, \eta_2, \eta_3\}$ begins to stabilize. At this same lag time, the second and third implied timescales become much flatter.

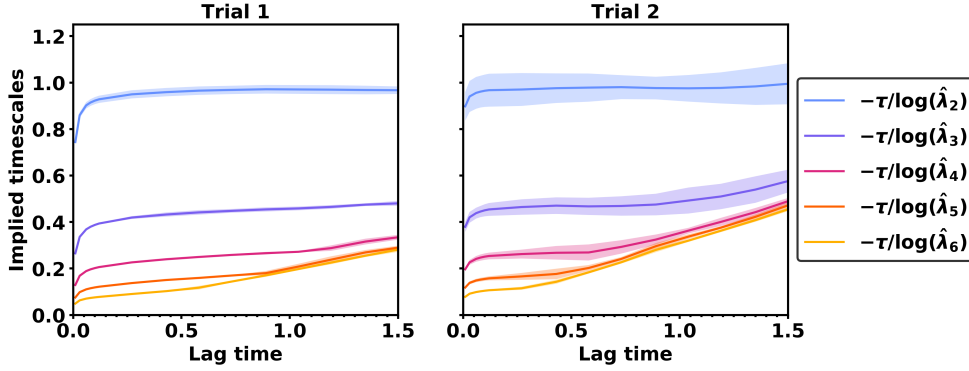


Figure 6: Implied timescales of the OU process.

We conclude that implied timescale analysis may be helpful for assessing VAC approximation error when the error is initially stabilizing. However, implied timescales should not be used to assess approximation error in the asymptotic regime or assess VAC estimation error. The VAC eigenvalue ratio provides a rigorous approach for assessing approximation error in the asymptotic regime, which can be computed at no additional cost compared to the implied timescales. The asymptotic estimation error is the only tool for measuring estimation error.

4.2. Varying the size of the subspace. In this second experiment, we apply VAC to estimate the eigenfunctions of the diffusion process

$$(4.3) \quad dX = -\frac{1}{2}\sigma\sigma^T\nabla U(X)dt + \sigma dW$$

where the potential U and the diffusion matrix σ are given by

$$(4.4) \quad U(x_1, x_2) = 4x_1^4 - 8x_1^2 + x_1 + 0.5x_2^2, \quad \sigma = \begin{pmatrix} 2 & 0 \\ -1 & \sqrt{3} \end{pmatrix}.$$

We simulate an equilibrium trajectory of length $T = 500$ and then apply VAC using the basis set $\{1, x_1, x_2, x_1^2, x_1x_2, x_2^2\}$.

We investigate how the accuracy changes when VAC is used to estimate two subspaces of different sizes: $\text{span}\{\eta_1, \eta_2\}$ and $\text{span}\{\eta_1, \eta_2, \eta_3\}$. When estimating $\text{span}\{\eta_1, \eta_2\}$, there is a wide range of lag times that all lead to low error levels. As seen in Figure 7, the total error decreases between lag times of $\tau = 0$ and $\tau = 0.2$, but it is nearly constant for all lag times between $\tau = 0.2$ to $\tau = 1.5$. In contrast, when estimating $\text{span}\{\eta_1, \eta_2, \eta_3\}$, the total error is V-shaped with a distinct minimum at the lag time $\tau = 0.2$. The error rises rapidly as the lag time is increased beyond $\tau = 0.2$ due to an upsurge in the estimation error.

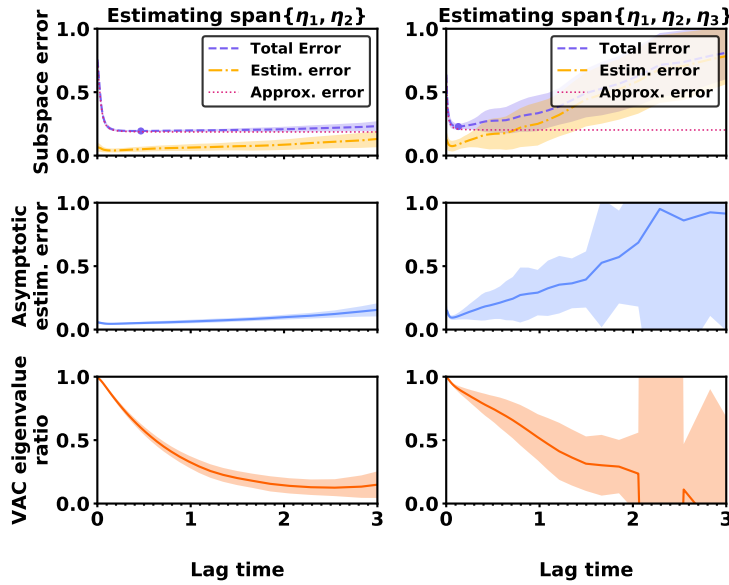


Figure 7: When the minimum condition number is 2.0, estimation error is low (left). When the minimum condition number is 9.5, estimation error is much higher (right).

What explains the different error profiles when estimating the subspace $\text{span}\{\eta_1, \eta_2\}$ versus $\text{span}\{\eta_1, \eta_2, \eta_3\}$? The explanation is not a difference in the data set or the basis set, since these factors remain the same when estimating the two subspaces. Rather, the increase in estimation error is due to the much higher condition number for the subspace $\text{span}\{\eta_1, \eta_2, \eta_3\}$. No matter how the lag time is selected, the condition number $(\lambda_4^\tau - \lambda_3^\tau)^{-1}$ is at least as high as 9.5. In contrast, when estimating the subspace $\text{span}\{\eta_1, \eta_2\}$, the minimum condition number $(\lambda_3^\tau - \lambda_2^\tau)^{-1}$ is just 2.0. Here we see a high condition number is associated with increased levels of estimation error and a stronger relationship between estimation error and lag time.

To avoid situations where the estimation error is uncontrollably high, VAC users should identify well-conditioned subspaces and focus on estimating these subspaces whenever possible. As shown in the VAC eigenvalue plot in Figure 8, eigenvalues for well-conditioned subspaces often visually stand apart from the rest of the eigenvalues. The large gap between the second and third VAC eigenvalue indicates a natural separation in timescales, which implies that $\text{span}\{\eta_1, \eta_2\}$ is a well-conditioned subspace.

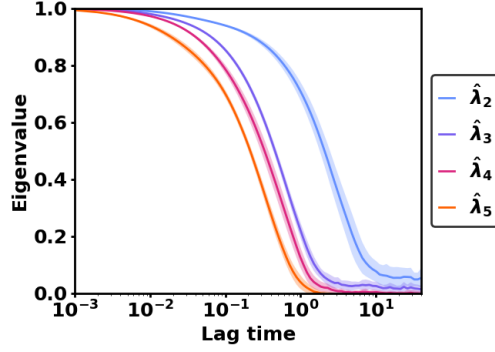


Figure 8: VAC eigenvalues.

5. Mathematical derivations. In this section, we prove the mathematical results presented in Theorem 3.4, Theorem 3.5, and Theorem 3.6.

5.1. Building mathematical intuition. Before proving Theorem 3.4, we identify the intuitive mathematical reason why idealized VAC estimates converge at long lag times. The intuitive reason for the convergence is revealed through a decomposition of the matrix $C(\tau)$. Applying the spectral decomposition (2.12), we find that each matrix entry $C_{ij}(\tau)$ has an exponentially decaying structure.

$$(5.1) \quad C_{ij}(\tau) = \langle \phi_i, T_\tau \phi_j \rangle = \sum_{l=1}^r e^{-\sigma_l \tau} \langle \eta_l, \phi_i \rangle \langle \eta_l, \phi_j \rangle + \mathcal{O}(e^{-\sigma_{r+1} \tau}) \quad \text{as } \tau \rightarrow \infty.$$

Thus, the matrix $C(\tau)$ is the sum of exponentially decaying rank-one matrices

$$(5.2) \quad C(\tau) = \sum_{l=1}^r e^{-\sigma_l \tau} \langle \eta_l, \vec{\phi} \rangle \langle \eta_l, \vec{\phi} \rangle^T + \mathcal{O}(e^{-\sigma_{r+1} \tau}) \quad \text{as } \tau \rightarrow \infty,$$

where we have used the shorthand $\langle \eta_l, \vec{\phi} \rangle$ to denote the vector with entries $\langle \eta_l, \phi_i \rangle$.

To approximate the behavior of idealized VAC at long lag times, we remove the smallest terms in the expansion (5.2) and replace $C(\tau)$ by the sum of k rank-one matrices

$$(5.3) \quad \sum_{l=1}^k e^{-\sigma_l \tau} \langle \eta_l, \vec{\phi} \rangle \langle \eta_l, \vec{\phi} \rangle^T.$$

When the rank- k approximation is used in place of $C(\tau)$, it results that the top k idealized VAC eigenfunctions $\gamma_1^\tau, \dots, \gamma_k^\tau$ span the subspace

$$(5.4) \quad \text{span}_{1 \leq i \leq k} q_i = \text{proj}[\Phi] \text{span}_{1 \leq i \leq k} \eta_i.$$

Therefore, the truncation argument helps intuitively explain the convergence of idealized eigenfunctions γ_i^τ to orthogonalized projections q_i as $\tau \rightarrow \infty$. Our proofs in [subsection 5.2](#), [subsection 5.3](#), and [subsection 5.4](#) essentially serve to justify the truncation argument and to provide rigorous bounds on the convergence behavior.

5.2. Convergence of idealized eigenvalues. In this section, we prove the convergence of idealized VAC eigenvalues

$$(3.12) \quad \frac{\lambda_i^\tau}{\langle \eta_i, q_i \rangle^2 e^{-\sigma_i \tau}} \rightarrow 1 \quad \text{as } \tau \rightarrow \infty$$

when there is a gap between σ_i and other σ_j values. To prove this result, our main tool is the min-max principle for self-adjoint operators [\[33\]](#):

Lemma 5.1. *Consider a quasi-compact self-adjoint operator*

$$(5.5) \quad A = \sum_{i=1}^r \lambda_i \text{proj}[\eta_i] + R.$$

Here, $\eta_1, \eta_2, \dots, \eta_r$ are orthonormal eigenfunctions of A with eigenvalues $\lambda_1 \geq \lambda_2 \geq \dots \geq \lambda_r$, and the spectrum of R lies in $(-\infty, \lambda_r)$. Then, for each $1 \leq k \leq r$,

$$(5.6) \quad \lambda_k(A) = \max_{\dim(H)=k} \min_{\eta \in H, \eta \neq 0} \frac{\langle \eta, A\eta \rangle}{\langle \eta, \eta \rangle}$$

Before applying the min-max principle, we derive two estimates.

Proposition 5.2. *For any $\phi \in \Phi \cap (\text{span}_{1 \leq i \leq k-1} q_i)^\perp$,*

$$(5.7) \quad \frac{\langle \phi, T_\tau \phi \rangle}{\langle \phi, \phi \rangle} \leq e^{-\sigma_k \tau} \langle \eta_k, q_k \rangle^2 + e^{-\sigma_{k+1} \tau}.$$

Proof. Calculate

$$(5.8) \quad \langle \phi, T_\tau \phi \rangle = \left\langle \phi, \left(\sum_{i=k}^r e^{-\sigma_i \tau} \text{proj}[\eta_i] + R_\tau \right) \phi \right\rangle$$

$$(5.9) \quad = e^{-\sigma_k \tau} \langle \eta_k, \phi \rangle^2 + \left\langle \phi, \left(\sum_{i=k+1}^r e^{-\sigma_i \tau} \text{proj}[\eta_i] + R_\tau \right) \phi \right\rangle$$

$$(5.10) \quad \leq e^{-\sigma_k \tau} \langle \eta_k, q_k \rangle^2 \langle q_k, \phi \rangle^2 + e^{-\sigma_{k+1} \tau} \langle \phi, \phi \rangle$$

$$(5.11) \quad \leq e^{-\sigma_k \tau} \langle \eta_k, q_k \rangle^2 \langle \phi, \phi \rangle + e^{-\sigma_{k+1} \tau} \langle \phi, \phi \rangle. \quad \blacksquare$$

Proposition 5.3. *Set $H_{1:k-1} = \text{span}_{1 \leq i \leq k-1} \eta_i$. Then for any $q \in \text{span}_{1 \leq i \leq k} q_i$,*

$$(5.12) \quad \frac{\langle q, T_\tau q \rangle}{\langle q, q \rangle} \geq e^{-\sigma_k \tau} \left(\langle \eta_k, q_k \rangle^2 - \frac{d_2^2(H_{1:k-1}, \Phi)}{e^{(\sigma_k - \sigma_{k-1})\tau} (1 - d_2^2(H_{1:k-1}, \Phi)) - \langle \eta_k, q_k \rangle^2} \right)$$

provided the denominator term is positive.

Proof. It suffices to consider the $\|q\| = 1$ case. Then, q can be decomposed as $q = aq' + bq_k$ where $a^2 + b^2 = 1$, $q' \in Q_{1:k-1}$, and $\|q'\| = 1$. It follows

$$(5.13) \quad \langle q, T_\tau q \rangle \geq \langle q, (e^{-\sigma_{k-1}\tau} \text{proj} [H_{1:k-1}] + e^{-\sigma_k\tau} \text{proj} [\eta_k]) q \rangle$$

$$(5.14) \quad = a^2 e^{-\sigma_{k-1}\tau} \|\text{proj} [H_{1:k-1}] q'\|^2 + e^{-\sigma_k\tau} \langle \eta_k, aq' + bq_k \rangle^2.$$

Thus, $\langle q, T_\tau q \rangle$ is bounded from below by the lowest eigenvalue of

$$(5.15) \quad M = e^{-\sigma_{k-1}\tau} \|\text{proj} [H_{1:k-1}] q'\|^2 \begin{pmatrix} 1 & 0 \\ 0 & 0 \end{pmatrix} + e^{-\sigma_k\tau} \begin{pmatrix} \langle \eta_k, q' \rangle^2 & \langle \eta_k, q' \rangle \langle \eta_k, q_k \rangle \\ \langle \eta_k, q' \rangle \langle \eta_k, q_k \rangle & \langle \eta_k, q_k \rangle^2 \end{pmatrix}.$$

For any symmetric real-valued matrix $M = \begin{pmatrix} a & b \\ b & c \end{pmatrix}$ with $a > c$, the lowest eigenvalue is at least as large as $c - b^2 / (a - c)$ [21]. We can check that

$$(5.16) \quad e^{-\sigma_{k-1}\tau} \left(1 - \|\text{proj} [H_{1:k-1}^\perp] q'\|^2 \right) \geq e^{-\sigma_{k-1}\tau} (1 - d_2^2(H_{1:k-1}, \Phi))$$

$$(5.17) \quad e^{-\sigma_k\tau} |\langle \eta_k, q' \rangle| \leq e^{-\sigma_k\tau} \|\text{proj} [H_{1:k-1}^\perp] q'\| \leq e^{-\sigma_k\tau} d_2(H_{1:k-1}, \Phi).$$

Therefore, the lowest eigenvalue of the matrix M is at least as large as

$$(5.18) \quad e^{-\sigma_k\tau} \langle \eta_k, q_k \rangle^2 - \frac{e^{-2\sigma_k\tau} d_2^2(H_{1:k-1}, \Phi)}{e^{-\sigma_{k-1}\tau} (1 - d_2^2(H_{1:k-1}, \Phi)) - e^{-\sigma_k\tau} \langle \eta_k, q_k \rangle^2}.$$

Proof of (3.12). Using the min-max principle and Proposition 5.2,

$$(5.19) \quad \lambda_k^\tau = \max_{\dim(S)=k, S \subseteq \Phi} \min_{\phi \in S} \frac{\langle \phi, T_\tau \phi \rangle}{\langle \phi, \phi \rangle} \leq e^{-\sigma_k\tau} \langle \eta_k, q_k \rangle^2 (1 + o(1))$$

as $\tau \rightarrow \infty$. Using the min-max principal and Proposition 5.3,

$$(5.20) \quad \lambda_k^\tau = \max_{\dim(S)=k, S \subseteq \Phi} \min_{\phi \in S} \frac{\langle \phi, T_\tau \phi \rangle}{\langle \phi, \phi \rangle} \geq \min_{q \in Q_{1:k}} \frac{\langle q, T_\tau q \rangle}{\langle q, q \rangle} \geq e^{-\sigma_k\tau} \langle \eta_k, q_k \rangle^2 (1 + o(1)).$$

5.3. Convergence of idealized subspaces. In this section, we prove the statement in Theorem 3.4 that idealized VAC subspaces converge

$$(3.13) \quad \text{span}_{j \leq i \leq k} \gamma_i^\tau \rightarrow \text{span}_{j \leq i \leq k} q_i, \quad \tau \rightarrow \infty$$

whenever there is a gap between $\{\sigma_j, \dots, \sigma_k\}$ and other σ_i values. To prove this result, our main tool is a well-known lemma due to Davis and Kahan [6].

Lemma 5.4. *Suppose A and B are self-adjoint operators and \mathcal{U} and \mathcal{W} are closed subspaces. If the spectrum of $\text{proj} [\mathcal{U}] A|_{\mathcal{U}}$ lies in the interval $[a, b]$ and the spectrum of $\text{proj} [\mathcal{W}] B|_{\mathcal{W}}$ lies in $(-\infty, a - \delta] \cup [b + \delta, \infty)$,*

$$(5.21) \quad \begin{aligned} & \delta \|\text{proj} [\mathcal{W}] \text{proj} [\mathcal{U}] \|_{\text{F}} \\ & \leq \|\text{proj} [\mathcal{W}] \text{proj} [\mathcal{U}] B \text{proj} [\mathcal{U}] - \text{proj} [\mathcal{W}] \text{proj} [\mathcal{U}] \text{proj} [\mathcal{W}] A\|_{\text{F}}. \end{aligned}$$

The Davis and Kahan lemma leads to the following error bound.

Proposition 5.5. *Assume that $\lambda_k^\tau > e^{-\sigma_{k+1}\tau}$. Then, the distance between subspaces $\Gamma_{1:k}^\tau = \text{span}_{1 \leq i \leq k} \gamma_i^\tau$ and $Q_{1:k} = \text{span}_{1 \leq i \leq k} q_i$ is bounded by*

$$(5.22) \quad d_F(\Gamma_{1:k}^\tau, Q_{1:k}) \leq \frac{e^{-\sigma_{k+1}\tau}}{2(\lambda_k^\tau - e^{-\sigma_{k+1}\tau})} d_F\left(\text{span}_{1 \leq i \leq k} \eta_i, \Phi\right).$$

Proof. The spectrum of $\text{proj}[\Phi \cap Q_{1:k}^\perp] T_\tau|_{\Phi \cap Q_{1:k}^\perp}$ lies in the interval $[0, e^{-\sigma_{k+1}\tau}]$, while the spectrum of $\text{proj}[\Gamma_{1:k}^\tau] T_\tau|_{\Gamma_{1:k}^\tau}$ lies in the interval $[\lambda_k^\tau, 1]$. Therefore, the spectral gap is at least $\lambda_k^\tau - e^{-\sigma_{k+1}\tau}$. We calculate

$$(5.23) \quad (\lambda_k^\tau - e^{-\sigma_{k+1}\tau}) \left\| \text{proj}[\Phi \cap Q_{1:k}^\perp] \text{proj}[\Gamma_{1:k}^\tau] \right\|_F$$

$$(5.24) \quad \leq \left\| \text{proj}[\Phi \cap Q_{1:k}^\perp] \text{proj}[\Gamma_{1:k}^\tau] T_\tau \text{proj}[\Gamma_{1:k}^\tau] \right. \\ \left. - \text{proj}[\Phi \cap Q_{1:k}^\perp] T_\tau \text{proj}[\Phi \cap Q_{1:k}^\perp] \text{proj}[\Gamma_{1:k}^\tau] \right\|_F$$

$$(5.25) \quad = \left\| \text{proj}[\Phi \cap Q_{1:k}^\perp] T_\tau \text{proj}[\Gamma_{1:k}^\tau] \right. \\ \left. - \text{proj}[\Phi \cap Q_{1:k}^\perp] T_\tau \text{proj}[\Phi \cap Q_{1:k}^\perp] \text{proj}[\Gamma_{1:k}^\tau] \right\|_F$$

$$(5.26) \quad = \left\| \text{proj}[\Phi \cap Q_{1:k}^\perp] T_\tau \text{proj}[Q_{1:k}] \text{proj}[\Gamma_{1:k}^\tau] \right\|_F$$

$$(5.27) \quad \leq \left\| \text{proj}[\Phi \cap Q_{1:k}^\perp] T_\tau \text{proj}[Q_{1:k}] \right\|_F$$

where we have used the fact that $\Gamma_{1:k}^\tau$ is an invariant subspace of $\text{proj}[\Phi] T_\tau \text{proj}[\Phi]$. Next, we introduce the subspace $H_{1:k} = \text{span}_{1 \leq i \leq k} \eta_i$, which is orthogonal to $\text{proj}[\Phi \cap Q_{1:k}^\perp]$. Then,

$$(5.28) \quad \left\| \text{proj}[H_{1:k}] \text{proj}[Q_{1:k}^\perp] \right\|_F = \left\| \text{proj}[H_{1:k}] \text{proj}[\Phi^\perp] \right\|_F = d_F\left(\text{span}_{1 \leq i \leq k} \eta_i, \Phi\right).$$

To complete the theorem, it is enough to show

$$(5.29) \quad \left\| \text{proj}[\Phi \cap Q_{1:k}^\perp] T_\tau \text{proj}[Q_{1:k}] \right\|_F \leq \frac{e^{-\sigma_{k+1}\tau}}{2} \left\| \text{proj}[H_{1:k}] \text{proj}[Q_{1:k}^\perp] \right\|_F.$$

To prove equation (5.29), we apply a useful property of the Frobenius norm. For any bounded linear operators A and B , if it is true that $\|Au\| \leq \|Bu\|$ for all u , then it follows that $\|A\|_F \leq \|B\|_F$ [11]. Using this property, it is sufficient to prove

$$(5.30) \quad \left\| \text{proj}[\Phi \cap Q_{1:k}^\perp] T_t q \right\| \leq \frac{e^{-\sigma_{k+1}\tau}}{2} \left\| \text{proj}[H_{1:k}^\perp] q \right\|$$

for all $q \in Q_{1:k}$. Moreover, it is sufficient to prove that

$$(5.31) \quad |\langle \phi, T_t q \rangle| \leq \frac{e^{-\sigma_{k+1}\tau}}{2}$$

for all $\phi \in \Phi \cap Q_{1:k}^\perp$ and $q \in Q_{1:k}$ with $\|\phi\| = \|\text{proj}[H_{1:k}^\perp] q\| = 1$. We observe

$$(5.32) \quad \left\| \text{proj}[H_{1:k}^\perp] (\phi \pm q) \right\|^2 = \left\| \phi \pm \text{proj}[H_{1:k}^\perp] q \right\|^2 = 2 \pm 2 \left\langle \text{proj}[H_{1:k}^\perp] \phi, q \right\rangle = 2.$$

Using the polarization identity and the fact that $H_{1:k}^\perp$ is an invariant subspace of T_τ , conclude

$$(5.33) \quad |\langle \phi, T_\tau q \rangle| = \left| \left\langle \text{proj}[H_{1:k}^\perp] \phi, T_\tau \text{proj}[H_{1:k}^\perp] q \right\rangle \right|$$

$$(5.34) \quad = \left| \frac{1}{4} \left\langle \text{proj}[H_{1:k}^\perp] (\phi + q), T_\tau \text{proj}[H_{1:k}^\perp] (\phi + q) \right\rangle - \frac{1}{4} \left\langle \text{proj}[H_{1:k}^\perp] (\phi - q), T_\tau \text{proj}[H_{1:k}^\perp] (\phi - q) \right\rangle \right|$$

$$(5.35) \quad \leq \frac{1}{2} \left\| \text{proj}[H_{1:k}^\perp] T_\tau \text{proj}[H_{1:k}^\perp] \right\|_2$$

$$(5.36) \quad \leq \frac{e^{-\sigma_{k+1}\tau}}{2}. \quad \blacksquare$$

[Proposition 5.5](#) allows us to verify the error bound [\(3.15\)](#) that was presented in [Theorem 3.4](#).

$$(5.37) \quad d_F^2 \left(\text{span}_{1 \leq i \leq k} \gamma_i^\tau, \text{span}_{1 \leq i \leq k} \eta_i \right)$$

$$(5.38) \quad = \left\| \text{proj}[\Phi^\perp] \text{proj}[H_{1:k}] \right\|_F^2 + \left\| \text{proj}[(\Gamma_{1:k}^\tau)^\perp] \text{proj}[\Phi] \text{proj}[H_{1:k}] \right\|_F^2$$

$$(5.39) \quad = \left\| \text{proj}[\Phi^\perp] \text{proj}[H_{1:k}] \right\|_F^2 + \left\| \text{proj}[(\Gamma_{1:k}^\tau)^\perp] \text{proj}[Q_{1:k}] \text{proj}[H_{1:k}] \right\|_F^2$$

$$(5.40) \quad \leq \left(1 + \frac{1}{4} \left| \frac{e^{-\sigma_{k+1}\tau}}{\lambda_k^\tau - e^{-\sigma_{k+1}\tau}} \right|^2 \right) d_F^2 \left(\text{span}_{1 \leq i \leq k} \eta_i, \Phi \right).$$

In addition, [Proposition 5.5](#) implies the convergence of idealized VAC eigenspaces. Indeed, if there is a gap between σ_k and σ_{k+1} , the right-hand side of equation [\(5.22\)](#) must vanish as $\tau \rightarrow \infty$. We must have

$$(5.41) \quad \text{span}_{1 \leq i \leq k} \gamma_i^\tau \rightarrow \text{span}_{1 \leq i \leq k} q_i \quad \text{as } \tau \rightarrow \infty.$$

Moreover, by applying the quadratic inequality in [Lemma 2.5](#), we verify that

$$(3.13) \quad \text{span}_{j \leq i \leq k} \gamma_i^\tau \rightarrow \text{span}_{j \leq i \leq k} q_i, \quad \text{as } \tau \rightarrow \infty$$

provided there is a gap between $\{\sigma_j, \dots, \sigma_k\}$ and other σ_i values.

5.4. Asymptotic error multiplier. In this section, we confirm the last part of [Theorem 3.4](#).

$$(3.14) \quad d_F \left(\text{span}_{1 \leq i \leq k} \gamma_i^\tau, \text{span}_{1 \leq i \leq k} q_i \right) = \left| \frac{\langle \eta_{k+1}, q_k \rangle}{\langle \eta_{k+1}, q_{k+1} \rangle} \right| \frac{\lambda_{k+1}^\tau}{\lambda_k^\tau} (1 + o(1)) \quad \text{as } \tau \rightarrow \infty,$$

provided that $e^{-\sigma_k \tau}$ and $e^{-\sigma_{k+1} \tau}$ are simple eigenvalues, and $\langle \eta_{k+1}, q_k \rangle \neq 0$.

Proof of (3.14). If there are fewer orthogonalized projection functions $(q_i)_{1 \leq i \leq p}$ compared to basis functions $(\phi_i)_{1 \leq i \leq n}$, we select additional functions $(q_i)_{p+1 \leq i \leq n}$ so that $(q_i)_{1 \leq i \leq n}$ is a complete orthonormal basis for Φ . Then $d_F(\Gamma_{1:k}, Q_{1:k})$ is given by

$$(5.42) \quad \left\| \text{proj} \left[\Phi \cap Q_{1:k}^\perp \right] \text{proj} [\Gamma_{1:k}] \right\|_F$$

$$(5.43) \quad = \left\| \left(\sum_{i=k+1}^n q_i \langle q_i, \cdot \rangle \right) \left(\sum_{j=1}^k \gamma_j^\tau \langle \gamma_j^\tau, \cdot \rangle \right) \right\|_F$$

$$(5.44) \quad = \left\| \sum_{i=k+1}^n \sum_{j=1}^k q_i \langle q_i, \gamma_j^\tau \rangle \langle \gamma_i^\tau, \cdot \rangle \right\|_F$$

$$(5.45) \quad = \left(\sum_{i=k+1}^n \sum_{j=1}^k \langle q_i, \gamma_j^\tau \rangle^2 \right)^{1/2}$$

The terms $\langle q_i, \gamma_j^\tau \rangle$ are determined by the eigenvalue equation

$$(5.46) \quad \lambda_j^\tau \langle q_i, \gamma_j^\tau \rangle = \langle q_i, T_\tau \gamma_j^\tau \rangle = \sum_{l=1}^n \langle q_i, T_\tau q_l \rangle \langle q_l, \gamma_j^\tau \rangle.$$

As $\tau \rightarrow \infty$, [Theorem 3.2](#) and the calculations in [Proposition 5.5](#) imply

$$(5.47) \quad 1/\lambda_j^\tau = \mathcal{O}(e^{\sigma_j \tau}) \quad \text{and} \quad |\langle q_i, T_\tau q_l \rangle| \leq \min \{e^{-\sigma_i \tau}, e^{-\sigma_l \tau}\}.$$

Setting $\epsilon = \min \{\sigma_{k+2} - \sigma_k, \sigma_{k+1} - \sigma_k\}$ and sending $\tau \rightarrow \infty$, we find

$$(5.48) \quad \left\| \text{proj} \left[\Phi \cap Q_{1:k}^\perp \right] \text{proj} [\Gamma_{1:k}] \right\|_F = |\langle q_{k+1}, \gamma_k \rangle| + \mathcal{O}(e^{-\epsilon \tau})$$

$$(5.49) \quad = \left| \frac{1}{\lambda_k^\tau} \sum_{l=1}^n \langle q_{k+1}, T_\tau q_l \rangle \langle q_l, \gamma_k^\tau \rangle \right| + \mathcal{O}(e^{-\epsilon \tau})$$

Lastly, as $\tau \rightarrow \infty$, we observe that $\gamma_k^\tau \rightarrow q_k$ and

$$(5.50) \quad \langle q_{k+1}, T_\tau q_k \rangle = \langle \eta_{k+1}, q_k \rangle \langle \eta_{k+1}, q_{k+1} \rangle e^{-\sigma_{k+1} \tau} (1 + o(1))$$

$$(5.51) \quad = \frac{\langle \eta_{k+1}, q_k \rangle}{\langle \eta_{k+1}, q_{k+1} \rangle} \lambda_{k+1}^\tau (1 + o(1))$$

This verifies (3.14). ■

5.5. Matrix perturbation theory. In this section, we show how matrix perturbation theory can be used to verify the error formulas in [Theorem 3.5](#).

Proof of Theorem 3.5. We first organize idealized VAC eigenvalues and coordinate vectors into matrices

$$(5.52) \quad \Lambda(\tau) = \text{diag} \{ (\lambda_1^\tau \quad \dots \quad \lambda_n^\tau) \}, \quad V(\tau) = (v_1(\tau) \quad \dots \quad v_n(\tau)).$$

Due to the normalization $\delta_{ij} = \langle \gamma_i^\tau, \gamma_j^\tau \rangle$, we must have

$$(5.53) \quad V(\tau)^T C(0) V(\tau) = I, \quad V(\tau)^T C(\tau) V(\tau) = \Lambda(\tau).$$

Thus, idealized VAC eigenfunctions γ_i^τ and eigenvalues λ_i^τ are the eigenfunctions and eigenvalues of the multiplication operator

$$(5.54) \quad \sum_{i,j=1}^n \gamma_i^\tau \Lambda_{ij}(\tau) \langle \gamma_j^\tau, \cdot \rangle = \sum_{i,j=1}^n \gamma_i^\tau \left(V(\tau)^{-1} C(0)^{-1} C(\tau) V(\tau) \right)_{ij} \langle \gamma_j^\tau, \cdot \rangle.$$

In contrast, VAC eigenfunctions $\hat{\gamma}_i^\tau$ and eigenvalues $\hat{\lambda}_i^\tau$ are eigenfunctions and eigenvalues of

$$(5.55) \quad \sum_{i,j=1}^n \gamma_i^\tau \left(V(\tau)^{-1} \hat{C}(0)^{-1} \hat{C}(\tau) V(\tau) \right)_{ij} \langle \gamma_j^\tau, \cdot \rangle.$$

As $\hat{C}(0) \rightarrow C(0)$ and $\hat{C}(\tau) \rightarrow C(\tau)$, we calculate

$$(5.56) \quad V(\tau)^{-1} \hat{C}(0)^{-1} \hat{C}(\tau) V(\tau)$$

$$(5.57) \quad = V(\tau)^T C(0) \hat{C}(0)^{-1} \hat{C}(\tau) V(\tau)$$

$$(5.58) \quad = V(\tau)^T \left[I + \left[\hat{C}(0) C(0)^{-1} - I \right] \right]^{-1} \hat{C}(\tau) V(\tau)$$

$$(5.59) \quad = V(\tau)^T \left[\hat{C}(\tau) - \left[\hat{C}(0) C(0)^{-1} - I \right] C(\tau) \right] V(\tau) \\ + \mathcal{O} \left(\left\| \hat{C}(0) - C(0) \right\|_F^2 + \left\| \hat{C}(\tau) - C(\tau) \right\|_F^2 \right)$$

$$(5.60) \quad = \Lambda(\tau) + \hat{L}(\tau) + \mathcal{O} \left(\left\| \hat{C}(0) - C(0) \right\|_F^2 + \left\| \hat{C}(\tau) - C(\tau) \right\|_F^2 \right),$$

where we have made repeated use of the identities (5.53). **Theorem 3.5** then follows by applying the first-order asymptotic formulas for the perturbation of eigenvalues and invariant subspaces when a diagonal matrix $\Lambda(\tau)$ is perturbed by a small error matrix $\hat{L}(\tau)$ (e.g., [14]). ■

5.6. Variance estimates. In this section we verify the results of **Theorem 3.6**.

Proof of Theorem 3.6. Following the definitions in **Theorem 3.5**, we set

$$(5.61) \quad \hat{L}_{li}(\tau) = v_l(\tau)^T \left[\hat{C}(\tau) - \lambda_i^\tau \hat{C}(0) \right] v_i(\tau), \quad 1 \leq l, i \leq n.$$

We will show the variables $\sqrt{T} \hat{L}_{li}(\tau)$ converge to a mean-zero multivariate normal distribution as $T \rightarrow \infty$. First decompose $\hat{L}_{li}(\tau)$ into three terms

$$(5.62) \quad \underbrace{\frac{\Delta}{T-\tau} \sum_{s=0}^{\frac{T-\tau}{\Delta}-1} F_{li}^\tau(X_{s\Delta}, X_{s\Delta+\tau})}_{A} + \underbrace{\lambda_i^\tau \frac{\Delta\tau}{T(T-\tau)} \sum_{s=\frac{\tau}{\Delta}}^{\frac{T-\tau}{\Delta}-1} \gamma_l^\tau(X_{s\Delta}) \gamma_i^\tau(X_{s\Delta})}_{B} \\ - \underbrace{\lambda_i^\tau \frac{\Delta(T-2\tau)}{2T(T-\tau)} \left[\sum_{s=0}^{\frac{\tau}{\Delta}-1} \gamma_l^\tau(X_{s\Delta}) \gamma_i^\tau(X_{s\Delta}) + \sum_{s=\frac{T-\tau}{\Delta}}^{\frac{T}{\Delta}-1} \gamma_l^\tau(X_{s\Delta}) \gamma_i^\tau(X_{s\Delta}) \right]}_C$$

We can bound terms B and C using

$$(5.63) \quad \text{Var}[B] \leq \left| \frac{\Delta\tau}{T(T-\tau)} \right|^2 \frac{T-2\tau}{\Delta} \text{Var}_\mu[\gamma_l^\tau(X_0) \gamma_i^\tau(X_0)]$$

$$(5.64) \quad \text{Var}[C] \leq \left| \frac{\Delta(T-2\tau)}{T(T-\tau)} \right|^2 \frac{2\tau}{\Delta} \text{Var}_\mu[\gamma_l^\tau(X_0) \gamma_i^\tau(X_0)]$$

As $T \rightarrow \infty$, $\text{Var}[B]$ is $\mathcal{O}(T^{-3})$ and $\text{Var}[C]$ is $\mathcal{O}(T^{-2})$, so both of these terms make an asymptotically negligible contribution to $\sqrt{T}\hat{L}_{li}(\tau)$.

A is the sample average of a stationary, mean-zero process $s \mapsto F_{li}^\tau(X_{s\Delta}, X_{s\Delta+\tau})$. Moreover the conditional expectations $\mathbb{E}[F_{li}^\tau(X_{s\Delta}, X_{s\Delta+\tau}) | X_0 = x]$ satisfy

$$(5.65) \quad \|\mathbb{E}[F_{li}^\tau(X_{s\Delta}, X_{s\Delta+\tau}) | X_0 = x]\| \leq C e^{-\sigma_2 s \Delta} \quad \forall s \geq 0,$$

for an appropriate constant $C < \infty$. Condition (5.65) is an asymptotic negligibility condition that guarantees the validity of the central limit theorem for the process $s \mapsto F_{li}^\tau(X_{s\Delta}, X_{s\Delta+\tau})$. Using the central limit theorem in [9, ch. 5], we verify

$$(5.66) \quad \sqrt{T}\hat{L}_{li}(\tau) \xrightarrow{\mathcal{D}} \mathcal{N}\left(0, \Delta \sum_{s=-\infty}^{\infty} \text{Cov}_\mu[F_{li}^\tau(X_0, X_\tau), F_{li}^\tau(X_{s\Delta}, X_{s\Delta+\tau})]\right), \quad T \rightarrow \infty$$

For simplicity, we have considered the asymptotic distribution of $\hat{L}_{li}(\tau)$. However, by the same approach we find that any linear combination of the $\hat{L}_{li}(\tau)$ variables has a limiting mean-zero normal distribution. By the Cramér-Wold theorem [13], the variables $\hat{L}_{li}(\tau)$ converge jointly to a mean-zero multivariate normal distribution. Theorem 3.6 follows by applying the asymptotic formulas (3.20) and (3.21). ■

6. Conclusions. In this paper, we have identified and bounded the major error sources of “the variational approach to conformational dynamics” (VAC) [26, 5, 25, 12]. VAC is frequently applied in biomolecular simulation studies to estimate the largest eigenvalues $e^{-\sigma_1\tau} \geq e^{-\sigma_2\tau} \geq \dots \geq e^{-\sigma_k\tau}$ for the Markov transition operator T_τ , along with the corresponding eigenfunctions $\eta_1, \eta_2, \dots, \eta_k$.

We have proved that VAC can identify subspaces of eigenfunctions $\text{span}_{j \leq i \leq k} \eta_i$ even when the state space is enormously high-dimensional. The convergence of VAC eigenfunction estimates is guaranteed under three conditions:

1. The values $\{\sigma_j, \dots, \sigma_k\}$ are separated from all other σ_i values by a spectral gap.
2. The library of basis functions $(\phi_i)_{1 \leq i \leq n}$ is very rich so that linear combinations of basis functions can fully represent η_1, \dots, η_k .
3. The data set is very large so that expectations $C_{ij}(0) = \mathbb{E}_\mu[\phi_i(X_0)\phi_j(X_0)]$ and $C_{ij}(\tau) = \mathbb{E}_\mu[\phi_i(X_0)\phi_j(X_\tau)]$ are evaluated with vanishing error.

VAC converges for any value of the lag time parameter $\tau > 0$, yet the choice of lag time can dramatically alter the speed of convergence. Hence, our main contribution is to prove error bounds that explicitly show how error depends on the lag time. These bounds provide a full theoretical justification for why limitations in the basis set contribute to the error at short lag times and limitations in the data set contribute to the error at long lag times.

Our numerical analysis approach is flexible, and it could be extended to algorithms besides VAC that estimate dynamical quantities of interest using trajectory data. A broadly useful approach involves decomposing the total error into approximation error and estimation error. Another useful approach involves identifying asymptotic formulas for the estimation error and then calculating the asymptotic estimation error using trajectory data. In future research, it is our goal to rigorously analyze the approximation and estimation error for other powerful algorithms used in biochemical simulation (e.g., [45]).

Lastly, while the main purpose of our work is to deepen theoretical understanding, we also provide practical diagnostic tools to assess VAC's accuracy and tune VAC's parameters. We present the VAC eigenvalue ratio as a tool to identify a range of lag times during which then approximation error stabilizes. We present the asymptotic estimation error as the first known measure that begins to provide error bars for VAC calculations. These diagnostic tools have direct relevance to the thousands of biochemical researchers using VAC, pointing the way toward a more streamlined lag time selection process and a more critical assessment of VAC's error for the future.

Acknowledgments. The authors would like to acknowledge helpful conversations with Chatipat Lorpai boon and John Strahan. RJW was supported by the National Science Foundation award DMS-1646339. EHT was supported by the Molecular Software Sciences Institute Software Fellows program. EHT, ARD, and JW were supported by the National Institutes of Health award R01GM109455. ARD and JW were supported by the National Institutes of Health award R35GM136381. JW was supported by the Advanced Scientific Computing Research Program within the DOE Office of Science through award DE-SC0020427. Computing resources were provided by the University of Chicago Research Computing Center.

REFERENCES

- [1] Y. F. ATCHADÉ AND F. PERRON, *On the geometric ergodicity of Metropolis-Hastings algorithms*, Statistics, 41 (2007), pp. 77–84.
- [2] L. BONINSEGNA, G. GOBBO, F. NOÉ, AND C. CLEMENTI, *Investigating molecular kinetics by variationally optimized diffusion maps*, Journal of Chemical Theory and Computation, 11 (2015), pp. 5947–5960.
- [3] N.-V. BUCHETE AND G. HUMMER, *Peptide folding kinetics from replica exchange molecular dynamics*, Physical Review E, 77 (2008), p. 030902.
- [4] W. CHEN, H. SIDKY, AND A. L. FERGUSON, *Nonlinear discovery of slow molecular modes using state-free reversible VAMPnets*, The Journal of Chemical Physics, 150 (2019), p. 214114.
- [5] J. D. CHODERA AND F. NOÉ, *Markov state models of biomolecular conformational dynamics*, Current opinion in structural biology, 25 (2014), pp. 135–144.
- [6] C. DAVIS AND W. M. KAHAN, *The rotation of eigenvectors by a perturbation. III*, SIAM Journal on Numerical Analysis, 7 (1970), pp. 1–46.
- [7] N. DJURDJEVAC, M. SARICH, AND C. SCHÜTTE, *Estimating the eigenvalue error of Markov state models*, Multiscale Modeling & Simulation, 10 (2012), pp. 61–81.
- [8] A. EDELMAN, T. A. ARIAS, AND S. T. SMITH, *The geometry of algorithms with orthogonality constraints*, SIAM journal on Matrix Analysis and Applications, 20 (1998), pp. 303–353.
- [9] P. HALL AND C. C. HEYDE, *Martingale limit theory and its application*, Academic press, 2014.
- [10] H. HIRAO, S. KOSEKI, AND H. TAKANO, *Molecular dynamics study of relaxation modes of a single polymer chain*, Journal of the Physical Society of Japan, 66 (1997), pp. 3399–3405.
- [11] R. A. HORN AND C. R. JOHNSON, *Matrix analysis*, Cambridge university press, 2012.
- [12] B. E. HUSIC AND V. S. PANDE, *Markov state models: From an art to a science*, Journal of the American

- Chemical Society, 140 (2018), pp. 2386–2396.
- [13] O. KALLENBERG, *Foundations of modern probability*, Springer Science & Business Media, 2006.
 - [14] M. KAROW AND D. KRESSNER, *On a perturbation bound for invariant subspaces of matrices*, SIAM Journal on Matrix Analysis and Applications, 35 (2014), pp. 599–618.
 - [15] S. KLUS, F. NÜSKE, P. KOLTAI, H. WU, I. KEVREKIDIS, C. SCHÜTTE, AND F. NOÉ, *Data-driven model reduction and transfer operator approximation*, Journal of Nonlinear Science, 28 (2018), pp. 985–1010.
 - [16] A. KNYAZEV, *Sharp a priori error estimates of the Rayleigh-Ritz method without assumptions of fixed sign or compactness*, Mathematical Notes, 38 (1985), pp. 998–1002.
 - [17] A. KNYAZEV, *New estimates for Ritz vectors*, Mathematics of computation, 66 (1997), pp. 985–995.
 - [18] B. LEIMKUHLER AND C. MATTHEWS, *Rational construction of stochastic numerical methods for molecular sampling*, Applied Mathematics Research eXpress, 2013 (2013), pp. 34–56.
 - [19] J. S. LIU, *Monte Carlo strategies in scientific computing*, Springer Science & Business Media, 2008.
 - [20] A. MARDT, L. PASQUALI, H. WU, AND F. NOÉ, *VAMPnets for deep learning of molecular kinetics*, Nature Communications, 9 (2018), p. 5.
 - [21] R. MATHIAS, *Quadratic residual bounds for the hermitian eigenvalue problem*, SIAM journal on matrix analysis and applications, 19 (1998), pp. 541–550.
 - [22] N. METROPOLIS, A. W. ROSENBLUTH, M. N. ROSENBLUTH, A. H. TELLER, AND E. TELLER, *Equation of state calculations by fast computing machines*, The Journal of Chemical Physics, 21 (1953), pp. 1087–1092.
 - [23] L. MOLGEDEY AND H. G. SCHUSTER, *Separation of a mixture of independent signals using time delayed correlations*, Physical Review Letters, 72 (1994), p. 3634.
 - [24] Y. NARITOMI AND S. FUCHIGAMI, *Slow dynamics in protein fluctuations revealed by time-structure based independent component analysis: the case of domain motions*, The Journal of Chemical Physics, 134 (2011), p. 02B617.
 - [25] F. NOÉ AND C. CLEMENTI, *Collective variables for the study of long-time kinetics from molecular trajectories: Theory and methods*, Current Opinion in Structural Biology, 43 (2017), pp. 141–147.
 - [26] F. NOÉ AND F. NUSKE, *A variational approach to modeling slow processes in stochastic dynamical systems*, Multiscale Modeling & Simulation, 11 (2013), pp. 635–655.
 - [27] F. NÜSKE, R. SCHNEIDER, F. VITALINI, AND F. NOÉ, *Variational tensor approach for approximating the rare-event kinetics of macromolecular systems*, The Journal of Chemical Physics, 144 (2016), p. 054105.
 - [28] F. NÜSKE, H. WU, J.-H. PRINZ, C. WEHMEYER, C. CLEMENTI, AND F. NOÉ, *Markov state models from short non-equilibrium simulations analysis and correction of estimation bias*, The Journal of Chemical Physics, 146 (2017), p. 094104.
 - [29] F. NSKE, B. G. KELLER, G. PÉREZ-HERNÁNDEZ, A. S. MEY, AND F. NO, *Variational approach to molecular kinetics*, Journal of Chemical Theory and Computation, 10 (2014), pp. 1739–1752.
 - [30] A. C. PAN AND B. ROUX, *Building markov state models along pathways to determine free energies and rates of transitions*, The Journal of chemical physics, 129 (2008), p. 064107.
 - [31] G. PÉREZ-HERNÁNDEZ, F. PAUL, T. GIORGINO, G. DE FABRITIIS, AND F. NOÉ, *Identification of slow molecular order parameters for Markov model construction*, The Journal of Chemical Physics, 139 (2013), p. 07B604.1.
 - [32] M. REED AND B. SIMON, *Methods of modern mathematical physics. 1: Functional analysis*, Academic Press, 1975.
 - [33] M. REED AND B. SIMON, *Methods of modern mathematical physics. 4: Analysis of operators*, Academic Press, 1978.
 - [34] C. W. ROWLEY, I. MEZIĆ, S. BAGHERI, P. SCHLATTER, AND D. S. HENNINGSON, *Spectral analysis of nonlinear flows*, Journal of fluid mechanics, 641 (2009), pp. 115–127.
 - [35] Y. SAAD, *Numerical methods for large eigenvalue problems: revised edition*, vol. 66, Siam, 2011.
 - [36] M. SARICH, F. NOÉ, AND C. SCHÜTTE, *On the approximation quality of Markov state models*, Multiscale Modeling & Simulation, 8 (2010), pp. 1154–1177.
 - [37] C. SCHÜTTE, A. FISCHER, W. HUISINGA, AND P. DEUFLHARD, *A direct approach to conformational dynamics based on hybrid Monte Carlo*, Journal of Computational Physics, 151 (1999), pp. 146–168.
 - [38] C. R. SCHWANTES AND V. S. PANDE, *Improvements in Markov state model construction reveal many non-native interactions in the folding of NTL9*, Journal of Chemical Theory and Computation, 9

- (2013), pp. 2000–2009.
- [39] A. SOKAL, *Monte Carlo methods in statistical mechanics: foundations and new algorithms*, in Functional integration, Springer, 1997, pp. 131–192.
 - [40] G. W. STEWART, *Stochastic perturbation theory*, SIAM review, 32 (1990), pp. 579–610.
 - [41] G. W. STEWART, *Matrix algorithms volume 2: eigensystems*, vol. 2, Siam, 2001.
 - [42] W. C. SWOPE, J. W. PITERA, AND F. SUITS, *Describing protein folding kinetics by molecular dynamics simulations. 1. Theory*, The Journal of Physical Chemistry B, 108 (2004), pp. 6571–6581.
 - [43] W. C. SWOPE, J. W. PITERA, F. SUITS, M. PITMAN, M. ELEFThERIOU, B. G. FITCH, R. S. GERMAIN, A. RAYSHUBSKI, T. C. WARD, Y. ZHESTKOV, ET AL., *Describing protein folding kinetics by molecular dynamics simulations. 2. Example applications to alanine dipeptide and a β -hairpin peptide*, The Journal of Physical Chemistry B, 108 (2004), pp. 6582–6594.
 - [44] H. TAKANO AND S. MIYASHITA, *Relaxation modes in random spin systems*, Journal of the Physical Society of Japan, 64 (1995), pp. 3688–3698.
 - [45] E. H. THIEDE, D. GIANNAKIS, A. R. DINNER, AND J. WEARE, *Galerkin approximation of dynamical quantities using trajectory data*, The Journal of Chemical Physics, 150 (2019), p. 244111.
 - [46] L. TONG, R.-W. LIU, V. C. SOON, AND Y.-F. HUANG, *Indeterminacy and identifiability of blind identification*, IEEE Transactions on circuits and systems, 38 (1991), pp. 499–509.
 - [47] S. M. ULAM, *A collection of mathematical problems*, vol. 8, Interscience Publishers, 1960.
 - [48] F. VITALINI, F. NOÉ, AND B. KELLER, *A basis set for peptides for the variational approach to conformational kinetics*, Journal of Chemical Theory and Computation, 11 (2015), pp. 3992–4004.
 - [49] M. O. WILLIAMS, I. G. KEVREKIDIS, AND C. W. ROWLEY, *A data-driven approximation of the Koopman operator: Extending dynamic mode decomposition*, Journal of Nonlinear Science, 25 (2015), pp. 1307–1346.
 - [50] H. WU, F. NÜSKE, F. PAUL, S. KLUS, P. KOLTAL, AND F. NOÉ, *Variational Koopman models: slow collective variables and molecular kinetics from short off-equilibrium simulations*, The Journal of Chemical Physics, 146 (2017), p. 154104.

7. Supplement.

7.1. Asymptotic estimation error. We describe the procedure for calculating the asymptotic estimation error in [Algorithm 7.1](#).

7.2. Figures for the Ornstein-Uhlenbeck process. Here we provide additional information about how [Figure 2](#) - [Figure 6](#) were generated. These figures show VAC applied to the Ornstein-Uhlenbeck process

$$(7.6) \quad dX = -X dt + \sqrt{2} dW$$

$$(7.7) \quad X_0 \sim N(0, 1).$$

The eigenfunctions of the transition operator T_t are the Hermite polynomials

$$(7.8) \quad 1, x, \frac{x^2 - 1}{\sqrt{2}}, \frac{x^3 - 3x}{\sqrt{6}}, \dots$$

with eigenvalues $1, e^{-t}, e^{-2t}, e^{-3t}, \dots$

The conditional distribution for the OU process is determined by

$$(7.9) \quad \text{Law}(X_t | X_0 = x) = N(xe^{-t}, 1 - e^{-2t}).$$

Therefore, we can simulate the OU process in discrete time using the exact evolution equations

$$(7.10) \quad X_0 \sim N(0, 1).$$

$$(7.11) \quad X_{t+\Delta} = e^{-\Delta} X_t + \xi_t, \quad \xi_t \sim N(0, 1 - e^{-2\Delta}).$$

Algorithm 7.1 Asymptotic estimation error

1. For $1 \leq l, i \leq n$, perform the following calculations.

- (a) Form the time series $\hat{F}_{li}^\tau(X_{r\Delta}, X_{r\Delta+\tau})$ for $r = 0, 1, \dots, \frac{T-\tau}{\Delta} - 1$, where the function $\hat{F}_{li}^\tau(x, y)$ is given by

$$(7.1) \quad \frac{\hat{\gamma}_l^\tau(x) \hat{\gamma}_i^\tau(y) + \hat{\gamma}_l^\tau(y) \hat{\gamma}_i^\tau(x)}{2} - \hat{\lambda}_i^\tau \frac{\hat{\gamma}_l^\tau(x) \hat{\gamma}_i^\tau(x) + \hat{\gamma}_l^\tau(y) \hat{\gamma}_i^\tau(y)}{2}.$$

- (b) For $s = 0, 1, \dots, \frac{T-\tau}{\Delta} - 1$, calculate the autocovariance terms $\hat{R}_{li}(s\Delta)$ given by

$$(7.2) \quad \frac{1}{\frac{T-\tau}{\Delta} - s} \sum_{r=0}^{\frac{T-\tau}{\Delta} - s - 1} \hat{F}_{li}^\tau(X_{r\Delta}, X_{r\Delta+\tau}) \hat{F}_{li}^\tau(X_{(r+s)\Delta}, X_{(r+s)\Delta+\tau})$$

- (c) Use the approach in [39, pg.143-145] to determine a truncation threshold K such that $\hat{R}_{li}(s\Delta) \approx 0$ for $s > K$, and set

$$(7.3) \quad \hat{V}_{li}(\tau)^2 = \frac{\Delta}{T} \left(1 + 2 \sum_{s=1}^K \hat{R}_{li}(s\Delta) \right).$$

2. Estimate eigenvalue estimation error or subspace estimation error using

$$(7.4) \quad \mathbb{E} \left| \hat{\lambda}_i^\tau - \lambda_i^\tau \right|^2 \approx \hat{V}_{ii}(\tau)^2$$

$$(7.5) \quad \mathbb{E} \left| d_F \left(\text{span}_{j \leq i \leq k} \hat{\gamma}_i^\tau, \text{span}_{j \leq i \leq k} \gamma_i^\tau \right) \right|^2 = \sum_{i=j}^k \sum_{\substack{l < j \\ \text{or } l > k}} \frac{\hat{V}_{li}(\tau)^2}{\left| \hat{\lambda}_l^\tau - \hat{\lambda}_i^\tau \right|^2}$$

When we apply VAC to the OU process, we use a basis of n indicator functions on disjoint intervals, namely,

$$(7.12) \quad \left\{ \mathbb{1}_{(-\infty, q_1)}, \mathbb{1}_{[q_1, q_2)}, \mathbb{1}_{[q_2, q_3)}, \dots, \mathbb{1}_{[q_{n-1}, \infty)} \right\}$$

The boundary points

$$(7.13) \quad q_0 = -\infty < q_1 < q_2 < \dots < q_{n-1} < q_n = \infty$$

are selected as follows:

1. First, we set $q_i = \Phi^{-1}(i/n)$ where

$$(7.14) \quad \Phi(x) = \int_{-\infty}^x \frac{e^{-y^2/2}}{\sqrt{2\pi}} dy$$

is the cumulative distribution function for a standard normal random variable and Φ^{-1} is the inverse cumulative distribution function, also called the quantile function.

2. Next, we set $q_i \leftarrow q_i + \epsilon$, where ϵ is an offset parameter that is always $\epsilon = 0.1$ in our figures. The offset parameter helps make our examples realistic, since it would typically be impossible in VAC applications to identify quantiles of the equilibrium distribution exactly.

Although many quantities involving the Ornstein-Uhlenbeck process can be calculated analytically, we used numerical quadrature to evaluate the integrals

$$(7.15) \quad \langle \eta_i, \phi_j \rangle = \int_{q_{j-1}}^{q_j} \eta_i(x) \frac{e^{-x^2/2}}{\sqrt{2\pi}} dx$$

and

$$(7.16) \quad \langle \phi_i, T_\tau \phi_j \rangle = \int_{q_{j-1}}^{q_j} \left[\Phi\left(\frac{q_i - xe^{-\tau}}{\sqrt{1 - e^{-2\tau}}}\right) - \Phi\left(\frac{q_{i-1} - xe^{-\tau}}{\sqrt{1 - e^{-2\tau}}}\right) \right] \frac{e^{-x^2/2}}{\sqrt{2\pi}} dx.$$

Remark 7.1. If the offset parameter were set to $\epsilon = 0$, the linear span Φ of the basis functions would decompose into even functions $\phi(x) = \phi(-x)$ and odd functions $\phi(x) = -\phi(-x)$. Thus, idealized VAC would decompose into one estimation problem for the even eigenfunctions $1, (x^2 - 1)/\sqrt{2}, \dots$ and an orthogonal estimation problem for the odd eigenfunctions $x, (x^3 - 3x)/\sqrt{6}, \dots$. The lag-time-dependent approximation error would no longer decay at an asymptotic $e^{-(\sigma_{k+1} - \sigma_k)\tau} = e^{-\tau}$ rate, since the conditions of part 3 of Theorem 3.4 would be violated. Rather, the lag-time-dependent approximation error would decrease at a faster $e^{-(\sigma_{k+2} - \sigma_k)\tau} = e^{-2\tau}$ rate. This observation suggests that symmetries of the transition operator can be exploited to reduce VAC's approximation error. However, a full exploration of symmetry considerations is outside the scope of the current paper.

7.3. Figures for the double well process. Here we provide additional information about how Figure 7 and Figure 8 were generated. These figures show VAC applied to the process

$$(7.17) \quad dX = -\frac{1}{2}\sigma\sigma^T\nabla U(X)dt + \sigma dW$$

where the potential U and the diffusion matrix σ are given by

$$(7.18) \quad U(x_1, x_2) = 4x_1^4 - 8x_1^2 + x_1 + 0.5x_2^2, \quad \sigma = \begin{pmatrix} 2 & 0 \\ -1 & \sqrt{3} \end{pmatrix}.$$

X_t is a double well process that spends long time periods in potential wells near $(-1, 0)$ and $(1, 0)$ with rare transitions between wells. We simulate X_t using the BAOAB-limit integrator presented in Leimkuhler and Matthews [18] with the timestep $\Delta = 10^{-4}$. We discard the first $t = 10$ time units of each trajectory to reduce equilibration bias.

To calculate reference values for the true eigenfunctions η_i and the idealized VAC matrices $C(\tau)$, we use the numerical PDE approach from appendix D of reference [45]. We first construct a grid from -2 to 2 in x and from -5 to 5 in y with grid spacing of $\epsilon = (6 \times 10^{-4})^{-1/2}$.

We next construct the transition matrix P for a hopping process on a grid:

$$(7.19) \quad P(x \pm \epsilon, y) = \frac{1}{6(1 + \exp[U(x \pm \epsilon, y) - U(x, y)])}$$

$$(7.20) \quad P(x, y \pm \epsilon) = \frac{1}{6(1 + \exp[U(x, y \pm \epsilon) - U(x, y)])}$$

$$(7.21) \quad P(x \pm \epsilon, y \pm \epsilon) = \frac{1}{6(1 + \exp[U(x \pm \epsilon, y \pm \epsilon) - U(x, y)])}$$

$$(7.22) \quad P(x \pm \epsilon, y \mp \epsilon) = 0$$

$$(7.23) \quad P(x, y) = 1 - P(x + \epsilon, y) - P(x - \epsilon, y) - P(x, y + \epsilon) - P(x, y - \epsilon).$$

In the $\epsilon \rightarrow 0$ limit, the action of $\frac{24}{\epsilon^2}(P - I)$ on smooth functions approximates the action of the infinitesimal generator L for the process X_t .

We calculate the eigenfunctions η_i using eigenfunctions of P . We calculate the idealized VAC matrix $C(\tau)$ using the approximation

$$(7.24) \quad C_{ij}(\tau) = \langle \phi_i, e^{L\tau} \phi_j \rangle$$

$$(7.25) \quad \approx \left\langle \phi_i, \left(I + \frac{\epsilon^2}{24} L \right)^{24\tau/\epsilon^2} \phi_j \right\rangle$$

$$(7.26) \quad \approx \vec{\phi}_i^T D_\mu P^{24\tau/\epsilon^2} \vec{\phi}_j,$$

where $\vec{\phi}_i$ is the vector of ϕ_i values evaluated at each gridpoint and D_μ is a diagonal matrix with the stationary measure associated with each gridpoint on the diagonal.

7.4. Rayleigh-Ritz approximation bounds. In this section, we re-derive the classic approximation bounds for the Rayleigh-Ritz method first presented in [16] and [17, pg. 992]. Our first step is to verify the inequality

$$(7.27) \quad 1 - d_2^2 \left(\text{span}_{1 \leq i \leq k} \eta_i, \Phi \right) \leq \frac{\lambda_k(\tau)}{e^{-\sigma_k \tau}} \leq 1$$

that appears in the statement of [Theorem 3.2](#).

Proof of equation (3.4). As in the proof of [Theorem 3.4](#), the upper bound

$$(7.28) \quad \lambda_k(\tau) = \max_{\dim(H)=k, H \subseteq \Phi} \min_{\eta \in H} \frac{\langle \eta, T_\tau \eta \rangle}{\langle \eta, \eta \rangle} \leq \max_{\dim(H)=k} \min_{\eta \in H} \frac{\langle \eta, T_\tau \eta \rangle}{\langle \eta, \eta \rangle} = e^{-\sigma_k \tau}$$

follows directly from the min-max principle.

The lower bound on $\lambda_k(\tau)$ follows trivially if $d_2(\text{span}_{1 \leq i \leq k} \eta_i, \Phi) = 1$. To handle the case $d_2(\text{span}_{1 \leq i \leq k} \eta_i, \Phi) < 1$, we define subspaces

$$(7.29) \quad H_{1:k} = \text{span}_{1 \leq i \leq k} \eta_i \quad \text{and} \quad Q_{1:k} = \text{proj}[\Phi] \text{span}_{1 \leq i \leq k} \eta_i.$$

For any $q \in Q_{1:k}$ with $\|q\| = 1$, we calculate

$$(7.30) \quad e^{\sigma_k \tau} \leq \frac{\langle T_\tau \text{proj} [H_{1:k}] q, \text{proj} [H_{1:k}] q \rangle}{\langle \text{proj} [H_{1:k}] q, \text{proj} [H_{1:k}] q \rangle} = \frac{\langle T_\tau \text{proj} [H_{1:k}] q, \text{proj} [H_{1:k}] q \rangle}{1 - \|\text{proj} [H_{1:k}^\perp] q\|^2}$$

$$(7.31) \quad \leq \frac{\langle \text{proj} [H_{1:k}] T_\tau \text{proj} [H_{1:k}] q, q \rangle + \langle \text{proj} [H_{1:k}^\perp] T_\tau \text{proj} [H_{1:k}^\perp] q, q \rangle}{1 - \|\text{proj} [H_{1:k}^\perp] \text{proj} [Q_{1:k}]\|^2}$$

$$(7.32) \quad = \frac{\langle T_\tau q, q \rangle}{1 - d_2^2(H_{1:k}, \Phi)}$$

We conclude that

$$(7.33) \quad (1 - d_2^2(H_{1:k}, \Phi)) e^{\sigma_k \tau} \leq \frac{\langle q, T_\tau q \rangle}{\langle q, q \rangle}, \quad \forall q \in Q_{1:k}.$$

The lower bound then follows by applying the min-max principle. ■

It remains to verify the inequality from [Theorem 3.2](#) that

$$(3.6) \quad 1 \leq \frac{d_F^2(\text{span}_{1 \leq i \leq k} \gamma_i^\tau, \text{span}_{1 \leq i \leq k} \eta_i)}{d_F^2(\text{span}_{1 \leq i \leq k} \eta_i, \Phi)} \leq 1 + \frac{\|\text{proj} [\Phi^\perp] T_\tau \text{proj} [\Phi]\|_2^2}{|e^{-\sigma_k \tau} - \lambda_{k+1}^\tau|^2}$$

whenever $e^{-\sigma_k \tau} > \lambda_{k+1}^\tau$.

Proof of equation (3.6). We define subspaces

$$(7.34) \quad H_{j:k} = \text{span}_{j \leq i \leq k} \eta_i \quad \text{and} \quad \Gamma_{j:k}^\tau = \text{span}_{j \leq i \leq k} \gamma_i^\tau.$$

Then it follows

$$(7.35) \quad \frac{d_F^2(\text{span}_{1 \leq i \leq k} \gamma_i^\tau, \text{span}_{1 \leq i \leq k} \eta_i)}{d_F^2(\text{span}_{1 \leq i \leq k} \eta_i, \Phi)} = \frac{\|\text{proj} [H_{1:k}] \text{proj} [(\Gamma_{1:k}^\tau)^\perp]\|_F^2}{\|\text{proj} [H_{1:k}] \text{proj} [\Phi^\perp]\|_F^2}$$

$$(7.36) \quad \leq 1 + \frac{\|\text{proj} [H_{1:k}] \text{proj} [\Gamma_{k+1:n}^\tau]\|_F^2}{\|\text{proj} [H_{1:k}] \text{proj} [\Phi^\perp]\|_F^2}$$

It remains to bound the distance between $H_{1:k}$ and the idealized VAC subspace $\Gamma_{k+1:n}^\tau$. To bound this distance, we apply the Davis-Kahan lemma as in the proof of [Theorem 3.4](#). The spectrum of $\text{proj} [H_{1:k}] T_\tau|_{H_{1:k}}$ lies in $[e^{-\sigma_k \tau}, \infty)$, while the spectrum of $\text{proj} [\Gamma_{k+1:n}^\tau] T_\tau|_{\Gamma_{k+1:n}^\tau}$ lies in $(-\infty, \lambda_{k+1}^\tau]$. Therefore, the spectral gap is at least $e^{-\sigma_k \tau} - \lambda_{k+1}^\tau$. It follows that

$$(7.37) \quad (e^{-\sigma_k \tau} - \lambda_{k+1}^\tau) \|\text{proj} [H_{1:k}] \text{proj} [\Gamma_{k+1:n}^\tau]\|_F$$

$$(7.38) \quad \leq \|\text{proj} [H_{1:k}] \text{proj} [\Gamma_{k+1:n}^\tau] T_\tau \text{proj} [\Gamma_{k+1:n}^\tau] - \text{proj} [H_{j:k}] T_\tau \text{proj} [H_{j:k}] \text{proj} [\Gamma_{k+1:n}^\tau]\|_F$$

$$(7.39) \quad = \|\text{proj} [H_{1:k}] \text{proj} [\Phi] T_\tau \text{proj} [\Gamma_{k+1:n}^\tau] - \text{proj} [H_{1:k}] T_\tau \text{proj} [\Gamma_{k+1:n}^\tau]\|_F$$

$$(7.40) \quad = \|\text{proj} [H_{1:k}] \text{proj} [\Phi^\perp] T_\tau \text{proj} [\Gamma_{k+1:n}^\tau]\|_F$$

$$(7.41) \quad \leq \|\text{proj} [H_{1:k}] \text{proj} [\Phi^\perp]\|_F \|\text{proj} [\Phi^\perp] T_\tau \text{proj} [\Phi]\|_2$$

where we have used the fact that $\Gamma_{k+1:n}^\tau$ is an invariant subspace of $\text{proj}[\Phi] T_\tau \text{proj}[\Phi]$ and $H_{1:k}$ is an invariant subspace of τ . \blacksquare

7.5. Sharper bounds on the lag-time-independent error. Here we prove an elegant bound on the lag-time-independent error.

Proposition 7.2. *The lag-time-independent error satisfies*

$$(7.42) \quad 1 \leq \frac{d_F(\text{span}_{j \leq i \leq k} q_i, \text{span}_{j \leq i \leq k} \eta_i)}{d_F(\text{span}_{j \leq i \leq k} \eta_i, \Phi)} \leq \frac{1}{\sqrt{1 - d_2^2(\text{span}_{1 \leq i \leq j-1}, \Phi)}}$$

Proof. To verify the upper bound, it is enough to prove

$$(7.43) \quad \left\| \text{proj} \left[Q_{j:k}^\perp \right] \eta \right\|^2 \leq \frac{\left\| \text{proj} \left[\Phi^\perp \right] \eta \right\|^2}{1 - \left\| \text{proj} \left[\Phi^\perp \right] \text{proj} \left[H_{1:j-1} \right] \right\|_2^2}$$

for all $\eta \in H_{j:k}$. Moreover, observing that

$$(7.44) \quad \left\| \text{proj} \left[Q_{j:k}^\perp \right] \eta \right\|^2 = \left\| \text{proj} \left[Q_{1:j-1} \right] \eta \right\|^2 + \left\| \text{proj} \left[\Phi^\perp \right] \eta \right\|^2,$$

it is enough to prove

$$(7.45) \quad \left\| \text{proj} \left[Q_{1:j-1} \right] \eta \right\|^2 \leq \frac{\left\| \text{proj} \left[\Phi^\perp \right] \eta \right\|^2 \left\| \text{proj} \left[\Phi^\perp \right] H_{1:j-1} \right\|_2^2}{1 - \left\| \text{proj} \left[\Phi^\perp \right] \text{proj} \left[H_{1:j-1} \right] \right\|_2^2}$$

If $\text{proj} \left[Q_{1:j-1} \right] \eta = 0$, then equation (7.45) follows trivially. Therefore, we consider the case where $\text{proj} \left[Q_{1:j-1} \right] \eta \neq 0$. Then, there is a function $\eta' \in H_{1:j-1}$ with

$$(7.46) \quad \text{proj} \left[\Phi \right] \eta' = \frac{\text{proj} \left[Q_{1:j-1} \right] \eta}{\left\| \text{proj} \left[Q_{1:j-1} \right] \eta \right\|}.$$

We can bound the norm of η' by observing

$$(7.47) \quad \left\| \eta' \right\|^2 = \left\| \text{proj} \left[\Phi \right] \eta' \right\|^2 + \left\| \text{proj} \left[\Phi^\perp \right] \eta' \right\|^2$$

$$(7.48) \quad \leq 1 + \left\| \text{proj} \left[\Phi^\perp \right] \text{proj} \left[H_{1:j-1} \right] \right\|_2^2 \left\| \eta' \right\|^2$$

This gives the norm bound

$$(7.49) \quad \left\| \eta' \right\|^2 \leq \frac{1}{1 - \left\| \text{proj} \left[\Phi^\perp \right] \text{proj} \left[H_{1:j-1} \right] \right\|_2^2}.$$

Using the norm bound and the orthogonality of $\eta \in H_{j:k}$ and $\eta' \in H_{1:j-1}$, we conclude

$$(7.50) \quad \left\| \text{proj} \left[Q_{1:j-1} \right] \eta \right\|^2 = \left\langle \text{proj} \left[\Phi \right] \eta, \text{proj} \left[\Phi \right] \eta' \right\rangle^2$$

$$(7.51) \quad = \left\langle \text{proj} \left[\Phi^\perp \right] \eta, \text{proj} \left[\Phi^\perp \right] \eta' \right\rangle^2$$

$$(7.52) \quad \leq \left\| \text{proj} \left[\Phi^\perp \right] \eta \right\|^2 \left\| \text{proj} \left[\Phi^\perp \right] \eta' \right\|^2$$

$$(7.53) \quad \leq \frac{\left\| \text{proj} \left[\Phi^\perp \right] \eta \right\|^2 \left\| \text{proj} \left[\Phi^\perp \right] H_{1:j-1} \right\|_2^2}{1 - \left\| \text{proj} \left[\Phi^\perp \right] \text{proj} \left[H_{1:j-1} \right] \right\|_2^2}. \quad \blacksquare$$